CHAPTER-2

Literature Review

2.1. Cancer

Cancer is a major cause of mortality: more than ten million people are diagnosed with the disease annually. Cancer is known to develop via a multistep carcinogenesis process entailing numerous cellular physiological systems such as cell signaling and apoptosis, making it a highly incomprehensible and complex disease (Reichert & Wenger, 2008; Zou, 2005). Initially, cancers start as localized diseases, but they are prone to spread to distant sites within the body, which makes cancer incurable. To date, cancer treatments have been performed on the basis of clinical and pathologic staging that is determined using morphologic diagnostic tools, such as conventional, radiological and histopathological examinations. The most common cancer treatments are restricted to chemotherapy, radiation and surgery (Singhal *et al.,* 2010). At present, however, the early recognition and treatment of cancer remain a technological bottleneck. Despite many advances in conventional treatment options such as chemotherapy and radiation, cancer therapy is still far from optimal treatment because it is plagued by some drawbacks. Frequent challenges encountered by current cancer therapies include nonspecific systemic distribution of antitumor agents, inadequate drug concentrations reaching the tumor site, intolerable cytotoxicity, limited ability to monitor therapeutic responses and development of multiple drug resistance (Das *et al.,* 2009; Parveen & Sahoo, 2006). Current diagnostic and prognostic classifications are insufficient to make predictions for successful treatment and patient outcome (Wang *et al.,* 2008).

2.2 Colorectal Cancer

Colorectal cancer (CRC) is one of the most common gastrointestinal tract malignancies as shown in Figure 2.1. It is the third cause of cancer-related death

in the western world (Jemal *et al.,* 2005) and affects about one million people every year throughout the world with a high mortality rate. CRC develops from a dysplasic precursor lesion, sporadically, in the context of high-risk hereditary conditions, or in the background of chronic inflammation.

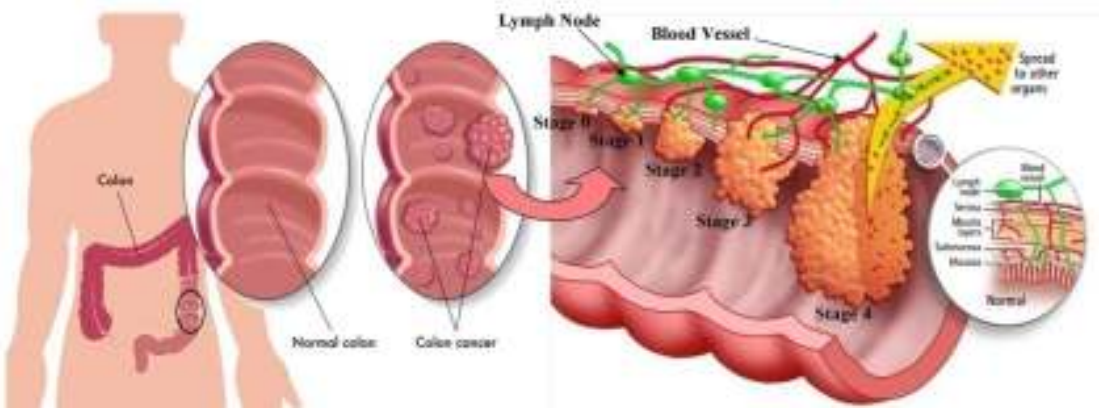

Figure 2.1 Schematic diagram of colorectal cancer from stage 0 to stage 4 (Adapted from Castellone *et al.,* 2006)

2.2.1 Molecular pathways of CRC: Role of inflammation and oxidative stress

Generally CRC arises as a result of sequential episodes of activating mutations in oncogenes, such as *ras*, and inactivating mutations, truncations or deletions in the coding sequence of several tumor suppressor genes, including p53 and adenomatous polyposis coli (APC), together with aberrant activity of molecules controlling genomic stability (Vogelstein & Kinzler, 2004). In particular, there are two main genomic instability that contribute to colon carcinogenesis: chromosomal instability (CIN) and microsatellity instability (MSI). The first results in abnormal segregation of chromosomes and abnormal DNA content (aneuploidy). The second involves loss of function genes that normally repair the mismatches between DNA base pairs that occur during the normal process of DNA replication in dividing cells (Itzkowitz, 2006).

Three genetic patterns have been categorized into the following groups of CRC: sporadic, inherited and familiar CRC. In hereditary cancer, such as familial adenomatous polyposis (FAP) and hereditary nonpolyposis colorectal cancer (HNPCC) some of these genetic mutations are inherited, while in sporadic cancer the mutations occur spontaneously. Particularly, the loss of a functional APC

protein is one of the earliest events occurring in sporadic CRC suggesting that APC may act as a gatekeeper of the colonic epithelium (Vogelstein & Kinzler, 2004). Loss of APC function allows β-catenin, a protein which plays a role in both cell adhesion and intracellular signaling, to gain access to the cell nucleus, where it complexes with specific transcription factors to activate genes implicated in proliferation, apoptosis and cell adhesion. APC also plays a role in epithelial migration and can localize at kinetochores, thereby participating in chromosome segregation during mitosis, which may contribute to the genetic instability and loss of epithelial polarity during the malignant transformation of colonic epithelia (Castellone *et al.,* 2006).

In addition to hereditable factors, cancer risk appears to be markedly influenced by a number of different factors including chronic inflammation. In effect, patients with inflammatory bowel disease (IBD) are among the highest risk groups for developing CRC. Increased risk of CRC in these patients becomes greater with increasing extent and duration of the disease (Itzkowitz, 2006). At present no genetic basis is able to explain the predisposition to CRC in those patients. Nevertheless, the main genomic instability that contributes to colon carcinogenesis in addition to MSI instability is CIN which results in damage of genetic material and consequently, loss of function of key tumor suppressor genes such as APC and p53 which express proteins that regulate growth and apoptosis. Loss of APC function occurs later normally in colitis-associated CRC. In normal cells, p53 is inactive through its joining to the MDM-2 protein, but several stimuli can activate it, resulting in anticancer responses: activation of genes involved in inhibition of cell cycle, apoptosis, chromosomic stability and inhibition of angiogenesis. Loss of p53 gene function occurs early and is supposed to be the crucial event that drives the adenoma to carcinoma (Itzkowitz, 2006; Burmer *et al.,* 1992).

Inflammation acts as a key regulator in all stages of carcinogenesis. Accumulating clinical and experimental evidence support a potent antitumourigenic efficacy of inhibiting the inducible isoform of COX-2 using nonsteroidal anti-inflammatory drugs and specific COX-2 inhibitors like

celecoxib in the setting of high-risk hereditary conditions. COX-2 is expressed after proinflammatory cytokines stimulation, oncogenes such as *ras* or *scr* or after hypoxia situations. In several types of cancer, particularly, gastric carcinoma and colon adenoma, COX-2 is up-regulated generating prostaglandins (PGs) that can promote cell growth, angiogenesis and suppression of immunity. Over expression of COX-2 is seen in up to 90% of colon carcinomas and 40% of colon adenomas. It is reasonable to assume that PGs produced by COX-2-expressing interstitial cells accelerate colon carcinogenesis (Itzkowitz & Yio, 2004; Zamuner *et al.,* 2005). Among them, a direct procarcinogenic role of PGE2 has been shown recently in various experimental animal models (Castellone *et al.,* 2006).

In addition to COX-2 inducible gene, iNOS and the interferon (IFN)-inducible genes are also increased in inflamed mucosa and remain elevated in colonic neoplasms (Ahn & Ohshima, 2001). iNOS is a calcium-independent nitric oxide (NO) synthase and responsible for production of large amounts of NO implicated in initiation, promotion and progression of tumors. The iNOS expression is induced by various inflammatory cytokines especially TNF-a, IFNc and bacterial cell wall products like LPS (Van der Woude *et al.,* 2004). Additionally, NO is able to cause DNA-damage and at the same time inhibits DNA repair mechanisms (Jaiswal *et al.,* 2001). Indeed, in chronic inflammation NO stimulates COX-2 activity and increases p53 mutations contributing to clonal cellular expansion and genomic instability.

Tumor cells are genetically unstable and produce structures which allow their cognition and destruction by the immune-surveillance system. Genetic and functional experiments indicate that tumor inflammatory infiltration primarily includes: T cells, specifically $CD4^+$ and $CD8^+$ and B cells as well as tumor-associated macrophages (TAMs), neutrophils, eosinophils, dendritic cells, natural killer cells and mast cells. They contribute to the development of carcinogenesis by producing a variety of cytokines such as TNF-α, proangiogenic factors and cytotoxic mediators including ROS and reactive nitrogen species (RNS) among others (Coussens & Werb, 2002; Dalerba *et al.,* 2003; Sun & Zhang, 2006). For

instance, leukocytes produce cytokines, angiogenic factors as well as matrix-degrading proteases that allow the tumor cells to proliferate, invade and metastasize.

Tumor-infiltrating lymphocytes secrete matrix metalloproteinase (MMP)-9 generating growth-promoting signals, angiogenesis and invasion (Egeblad & Werb, 2002). MMPs are members of the zinc-dependent endo-peptidases which have been implicated in the degradation of extracellular matrix. MMP-2 and MMP-9 are often over expressed in various cancers (Zucker & Vacirca, 2004). Their specific inhibitors also play a major regulatory role in matrix reorganization and the initiation of angiogenesis (Schnaper *et al.,* 1993). Thus, the over expression of MMPs may be one part of the multistep process that leads to neoplastic cell proliferation and metastasis.

Gap-junction intercellular communication (GJIC) is essential for maintaining homeostasis via the modulation of cell proliferation and differentiation in multicellular organisms (Kumar & Gilula, 1996). Normal fibroblasts and epithelial cells have functional GJIC, while the majority of tumor cells have dysfunctional homologous or heterologous GJIC. Thus, the augmentation of GJIC and inhibition of COX-2 and MMPs are considered examples of interesting biomarkers concerning in blocking tumor promotion and tumor progression in carcinogenesis.

It is logical to assume that factors associated with inflammation such as oxidative stress, contribute to neoplastic transformation. ROS mainly the superoxide anion, which is converted to the secondary oxidant H_2O_2 by superoxide dismutase, and RNS, mostly NO and its metabolite peroxynitrite, can interact with DNA in proliferating epithelium resulting in permanent genomic alterations including point mutations, deletions or rearrangements. In addition, ROS may contribute to the p53 mutations and can functionally impair the protein components of the DNA mismatch repair system (Itzkowitz, 2006). Likewise, exacerbating DNA injury induces the macrophage infiltration inhibitory factor (MIF) expression from macrophages and T lymphocytes. MIF is a potent cytokine

that overcomes p53 function by suppressing its transcriptional activity (Hudson *et al.,* 1999).

ROS can interfere with normal cellular signaling cascades by influencing the activation or expression of transcription factors and upstream kinase, especially NF-jB and activator protein-1 (AP-1). NF-jB can modulate the genes involved in tumor cell proliferation, invasion and angiogenesis; these include the cell adhesion molecules, COX-2, iNOS, MMP-9, MMP-2, chemokines and inflammatory cytokines among others. Also, the activation of NF-jB can suppress apoptosis, thus promoting chemoresistance and tumourigenesis (Bharti & Aggarwal, 2002). In relation to AP-1, it is known to play a main role in not only the proliferation of initiated cells but also in the metastasis of tumor cells. In fact, activation of AP-1 induces the expression of target genes for instance, COX-2, urokinase-type plasminogen activator, Fos, MMP-9, cyclin D1 and vascular endothelial growth factor (VEGF) that are involved in neoplastic transformation, tumour progression, metastasis and angiogenesis (Lee & Lee, 2006). The components of NF-jB and AP-1 are activated by the three major groups of MAPKs in mammalian cells, the extracellular signal related kinases (ERK), the c-Jun NH2-terminal kinases (JNK) and p38 MAPK that are activated by phosphorylation. NF-jB, AP-1 and associated MAPK signal transduction pathways are believed to be crucial in cell transformation and tumor promotion, and hence have been proposed as targets for chemopreventive agents (Kundu & Surh, 2004).

Recent investigations suggest the participation of the peroxisome proliferator-activated receptor gamma (PPARc) in the pathophysiology of inflammatory and immune responses possibly through inhibition of the MAPKs pathway or the activation of the NF-jB. In colon tumor tissue, PPARc expression has been detected in several studies using clinical samples. Activation of PPARc leads to cell differentiation and apoptosis. Also, PPARc ligands have been shown to be potent inhibitors of angiogenesis, a process necessary for tumor growth and metastasis, and protect against cellular transformation. Further work is needed to establish in detail the anti-proliferative and pro-differentiation

mechanisms of PPARc activators and their expedient evaluation in the clinical management of IBD-associated CRC (Bull, 2003; Alarcon de la Lastra *et al.,* 2004).

2.2.2 Epidemiology

2.2.2.1 Risk Factors

Most cases of CRC arise sporadically. Risk factors include increasing age, male sex, previous colonic polyps, or previous CRC and environmental factors such as red meat, high-fat diet, inadequate intake of fibre, obesity, sedentary lifestyle, diabetes mellitus, smoking, and high consumption of alcohol. Inflammatory bowel disease (ulcerative colitis and Crohn's disease) accounts for roughly two-thirds of the incidence (Von roon *et al.,* 2007; Eaden *et al.,* 2001) and the risk increases with duration of illness (2% at 10 years, 18% by 30 years) and severity and extent of inflammation (Itzkowitz & Harpaz, 2004). Although colitis-associated CRC has many of the same molecular carcinogenic mechanisms as has sporadic cancer, with similar frequencies of chromosomal (about 85%) and microsatellite instability (about 15%), there are important molecular differences (Triantafi *et al.,* 2009).

Of the hereditary syndromes, the frequencies for inherited syndromes are as follows; the Lynch syndrome, also known as hereditary non-polyposis colorectal cancer, occurs in roughly one in 300 people with CRC. Familial adenomatous polyposis is much less frequent, and arises in about one in 7000 people affected by CRC, whereas MYH-associated polyposis occurs in about one in 18000 individuals with CRC. All familial cases of CRC of the syndrome type account for nearly 6% of cases-namely, 3% of those with Lynch syndrome, 2% with familial CRC non-Lynch syndrome, and about 1% constitute all of the others, including the TACSTD1 deletion of MSH2. At this time, there is no reliable quantitative estimate of the frequency of TACSTD1 deletion of MSH2 in Lynch syndrome.

2.2.2.2 Genetic epidemiology: Lynch syndrome as model

More than a fifth of patients with CRC might have a familial component, and about 3% of cases will develop Lynch syndrome (Hampel *et al.,* 2008), which is the most common hereditary syndrome associated with this cancer (panel 1). Less than 1% of cases will have familial adenomatous polyposis or one of the hereditary syndromes of hamartomatous polyposis (Bussey, 1975; Bulow *et al.,* 1996). At least 20% of cases of CRC are familial (defined by two or more first-degree relatives with this cancer). Although this familial category remains aetiologically elusive, it is estimated to have a two-fold to three-fold greater risk than has the general population. Type X familial CRC, a new susceptibility category, meets the Amsterdam criteria (Vasen *et al.,* 1999) for Lynch syndrome but lacks the molecular genetic features (Lindor *et al.,* 2005; Llor *et al.,* 2005). The Amsterdam criteria (Vasen *et al.,* 1999) and Bethesda guidelines (Umar *et al.,* 2004) are widely used as clinical screening methods for assessment of risk (panel 2).

Panel 1: Cardinal features of Lynch syndrome (hereditary non-polyposis CRC)

- Autosomal dominant inheritance pattern of syndrome cancers in the family pedigree.
- Onset of CRC at a younger average age than in the general population: average age of 45 years in individuals with Lynch syndrome versus 63 years in the general population.
- Proximal (right-sided) colonic cancer predilection: 70-85% of CRC in people with Lynch syndrome are proximal to the splenic flexure.
- Accelerated carcinogenesis (small adenomas can develop into carcinomas quickly): within 2-3 years in Lynch syndrome versus 8-10 years in the general population.

- High risk of additional CRC: 25-30% of patients having surgery for a cancer associated with Lynch syndrome will have a second primary CRC within 10 years of surgical resection if the surgery was less than a subtotal colectomy.
- Increased risk of malignancy at specific extra colonic sites: (Watson *et al.,* 2008; Barrow *et al.,* 2009) endometrium (40-60% lifetime risk in carriers of mutation); ovary (12-15% lifetime risk in mutation carriers); stomach (increased risk in Oriental families, reason not known); small bowel; hepatobiliary tract; pancreas; upper uroepithelial tract (transitional cell carcinoma of the ureter and renal pelvis); and brain (in Turcot's syndrome, a variant of Lynch syndrome).
- Sebaceous adenomas, sebaceous carcinomas, and multiple keratoacanthomas in Muir-Torre's syndrome, a variant of Lynch syndrome.
- Pathology of colorectal cancer is often poorly diff erentiated, with an excess of mucoid and signet cell features, a Crohn's-like reaction, and an excess of infi ltrating lymphocytes within the tumor.
- Increased survival when compared by stage in non-Lynch-syndrome-associated CRC.
- The requirement for diagnosis is the identification of a germline mutation in a mismatch repair gene (most commonly MLH1, MSH2, or MSH6) that segregates in the family i.e., members who have the mutation have a much higher rate of syndrome related cancers than do those who do not have the mutation.

Panel 2: Revised Bethesda guidelines and Amsterdam criteria for identification of patients at risk of developing Lynch syndrome

Traditionally, one Bethesda criterion or all Amsterdam criteria should be met to potentially identify individuals at risk of Lynch syndrome.

Bethesda guidelines:

- Colorectal cancer diagnosed in a patient who is younger than 50 years
- Presence of synchronous, metachronous colorectal, or other tumors associated with Lynch syndrome, irrespective of age
- Diagnosis of CRC with histologically high-level microsatellite instability in a patient younger than 60 years
- CRC diagnosed in one or more first-degree relatives with a Lynch syndrome-associated tumor, with one of the cancers diagnosed before age 50 years
- CRC diagnosed in two or more first-degree or second-degree relatives with Lynch-syndrome-related tumors irrespective of age

Amsterdam I and II criteria:

- One individual diagnosed with CRC (or extra colonic Lynch-syndrome associated tumors) before age 50 years
- Three affected relatives, one a first-degree relative of the other two
- Two successive affected generations
- Familial adenomatous polyposis should be excluded
- Tumors should be verified by pathological examination

2.2.3 Screening of CRC

Survival rates in individuals with CRC have increased substantially in the past few years, possibly as a result of early diagnosis and improved treatment. Although substantial information about risk factors exists, about 75% of diagnoses are in patients with no apparent risk factors other than older age. 5-year survival is still less than 60% in most European countries (Verdecchia *et al.,* 2007). Population screening therefore continues to offer the best prospects for reduction in mortality rates.

The aim of screening for CRC is to prevent the development of advanced cancers through detection of localized cancers or premalignant adenomas, from which at least 80% of cancers are thought to arise. Several technologies exist. Those that are used to target cancers early reduce mortality rates, but cause a temporary increase in incidence rates as cancers are typically diagnosed at screening 2-3 years earlier than in symptomatic cases. These tests need to be offered at least biennially, which has implications for costs and compliance rates. Tests that are used to detect adenomas can be offered less frequently and because these tests should reduce incidence rates of CRC, they also reduce the costs of treatment and thereby, of the screening programme (Tappenden *et al.,* 2007; Loeve *et al.,* 2000). However, since most adenomas do not develop into symptomatic cancers, screening for them can result in over treatment, which can increase the risk of complications.

The guaiac-based faecal occult blood test is the most extensively studied, but possibly least sensitive, screening method. Several randomized trials and a Cochrane review (Towler *et al.,* 1998) have provided high-quality evidence that this test, if offered every 2 years, has the potential to reduce mortality rates associated with CRC by 16%. For this home-test kit, two samples are collected from three consecutive stools and sent for processing in an accredited laboratory. Collection of one stool sample by a physician during digital rectal examination is ineffective and is strongly discouraged (Collins *et al.,* 2005). Investigation by colonoscopy is recommended if a specific number of the test cards are positive; the exact number varies according to local practice (Steele *et al.,* 2001; Benson *et al.,* 2008). Several countries have introduced screening with the faecal occult blood test (Benson *et al.,* 2008). Costs have been assessed in the European and US contexts, and were well below the commonly used threshold of US$50000 per life-year gained (Tappenden *et al.,* 2007; Pignone *et al.,* 2002). Immunochemical faecal occult blood tests have several improved features compared with the standard test. They are not subject to interference from animal blood in the diet, only one or two stool samples are needed, and they are more sensitive for detection of CRC and advanced adenomas, though at the

expense of lower specificity (Whitlock *et al.,* 2008). Some tests can be automated, and the cutoff for positivity can be adjusted according to available endoscopy resources (Castiglione *et al.,* 2002).

2.2.4 Diagnosis and staging

CRC is diagnosed on the basis of the results of colonoscopy or sigmoidoscopy with tumor biopsy. Treatment strategy is guided by adequate staging. The pretreatment workup of a newly diagnosed cancer includes physical examination, a complete colonoscopy to rule out metachronous tumor and CT of the chest, abdomen, and pelvis to identify metastatic disease (Mauchley *et al.,* 2005).

CT colonography is valuable for precise localization of the tumor and can help surgical approaches, especially in patients who are candidates for laparoscopic resection. It might also be used to identify other colonic lesions or polyps that are not detected at colonoscopy, for instance because of an obstructive lesion (Mainenti *et al.,* 2005; Copel *et al.,* 2007; Morrin *et al.,* 1999). Routine use of PET with the 18-fluoro-2-deoxy-D-glucose (FDG-PET) is not recommended at the time of initial diagnosis. In patients with rectal cancer, assessment of local tumor extension is essential for optimum treatment. High resolution MRI can be used to accurately measure the spread of tumor in the surrounding mesorectum, and to assess the circumferential resection margin between the edge of tumor and the fascia recti (Brown *et al.,* 2003). Measurement of the depth of invasion in the bowel wall with endorectal ultrasound is particularly useful for early rectal cancers (Bipat *et al.,* 2004).

2.2.5 Surgery

For CRC, total resection of the tumor should be done with adequate margins, and lymph adenectomy. Distal margins of 5 cm or more are recommended. At least 12 lymph nodes should be taken and analyzed to allow appropriate nodal staging (Le Voyer *et al.,* 2003; Chang *et al.,* 2007; Prandi *et al.,* 2002); analysis of fewer than ten nodes might under stage the tumor

(Cunningham *et al.,* 1998). En-bloc resection of invaded adjacent organs might be needed for T4 tumors to obtain R0 resection (no evidence of microscopic cancer at the margins). Surgical resection of the rectum for invasive rectal cancer should include total excision of the mesorectum (TME) with adequate circumferential and distal margins, and inferior mesenteric lymph adenectomy. TME is associated with a reduced risk of local recurrence whether or not combined with preoperative radiotherapy or chemo radiotherapy (Peeters *et al.,* 2007; Bosset *et al.,* 2006). Sphincter-saving surgery is feasible in most patients with mid and low rectal cancers if the distal margin is 1 cm or more. Intestinal continuity can be restored with colorectal or coloanal anastomosis according to the level of the tumor. For very low tumors, TME can be combined with resection of the internal sphincter of the anus without increasing the rate of local recurrence (Rullier *et al.,* 2005; Chamlou *et al.,* 2007). Abdominoperineal resection is a valuable alternative for very low tumors (Cornish *et al.,* 2007). Functional results after TME are associated with the level of the anastomosis. Risk of faecal incontinence is increased in patients with very low coloanal anastomosis, particularly after preoperative radiation (Bretagnol *et al.,* 2004; Van *et al.,* 2002).

2.2.6 Radiation treatment for CRC

Chemoradiation and short-course radiotherapy have been the main preoperative strategies assessed in randomized studies. Short-course preoperative radiation in patients with rectal cancer resulted in a survival advantage for the total treatment group in a Swedish trial (Birgisson *et al.,* 2005). Despite TME, the local recurrence rate with no depositive disease was 21% in the Dutch CKVO 95-04 trial. Therefore patients with node-positive tumors need adjuvant radiation. The challenge is accurate identification of positive nodes to allow proper selection of patients for preoperative treatment. In the randomized study by Bujko and colleagues (Peeters *et al.,* 2007), patients given chemoradiation compared with radiation (5 Gy×5) had a significantly lower incidence of positive circumferential resection margin (4% vs 13%), but no significant difference in local failure (14% vs 9%) or 4-year survival (66% vs 67%). Furthermore, although the rate of pathological complete response was

much higher (16% vs 1%), the incidence of sphincter preservation was not increased. However, because the number of patients (n=316) was small, surgeons were not encouraged to modify the operation on the basis of tumor response, and there was a lack of central review of the quality of the radiotherapy.

2.2.7 Adjuvant treatment for early stage CRC

In node-positive (stage III) disease, administration of adjuvant fluorouracil for 6 months reduces the risk of death by 30%, which is equivalent to an additional 10-15% survival gain. The alternative oral fluoropyrimidine, capecitabine, has shown similar efficacy to fluorouracil alone (Twelves *et al.,* 2005). The establishment of 3-year disease-free survival as a validated surrogate for 5-year overall survival (Sargent *et al.,* 2005; Sargent *et al.,* 2007) and primary endpoint has expedited the timely reporting of adjuvant trials and uptake of effective treatments. However, the magnitude of benefit in disease-free survival is not necessarily matched by that in overall survival because of various factors (Sargent *et al.,* 2007). Oxaliplatin (a third-generation platinum) added to infused fluorouracil versus infuse fluorouracil alone improved 3-year disease-free survival by 7% in the MOSAIC study (Andre *et al.,* 2004), leading to a 2·5% gain in overall survival at 6 years for stage II and III disease, and a survival increment of 4·2% in stage III alone (Andre *et al.,* 2009). Results for disease-free survival were replicated in the NSABP C-07 study of fluorouracil and oxaliplatin (Kuebler *et al.,* 2007). In the XELOXA study of oral capecitabine plus oxaliplatin versus fluorouracil and folinic acid (stage III disease), there was an improvement in 3-year disease-free survival (70·9% vs 66·5%, hazard ratio 0·80, p=0·0045) but a non-significant 5 year benefit in overall survival (3·4%). The choice between one drug (intravenous fluorouracil or oral capecitabine) or two will depend on the patient's fitness or preference, potential for compliance, and toxicity considerations-eg, hand-foot syndrome with capecitabine, and risk of permanent peripheral sensory neuropathy with oxaliplatin (15·5% all grades of peripheral sensory neuropathy at 48 months after treatment) (Andre *et al.,* 2009), with patient-reported improvement in hand peripheral sensory neuropathy but

worsening of foot numbness, tingling, or discomfort by 18 months (Land *et al.,* 2007). Results from the MOSAIC study did not suggest a survival benefit with adjuvant oxaliplatin and fluorouracil in patients older than 65 years, a finding supported for individuals older than 70 years in an analysis of the ACCENT group database of more than 12,500 patients (17% older than 70 years) given adjuvant treatment in six randomized studies (including NSABP C-07 and MOSAIC) (Jackson McCleary *et al.,* 2009). These data and toxicity considerations imply fluoropyrimidine monotherapy might be considered in older patients with stage III colorectal cancer. Irinotecan added to fluorouracil did not significantly improve disease-free or overall survival (Saltz *et al.,* 2007), although there was a non-significant improvement with combination treatment in the PETAAC-3 trial (Van *et al.,* 2009). Adjuvant chemotherapy for node-negative (stage II) colon cancer (40% of resected cancers) has been controversial because of the small gains in survival for this subgroup in studies in which patients with stage II and III cancer were combined, although high-risk patients with stage II tumors (T4 tumors, obstructing presentation, poor differentiation, extramural venous invasion, fewer than 10-12 harvested lymph nodes, indeterminate or positive resection margins) are often offered treatment (Cunningham & Starling, 2007). However, in the QUASAR study of 3239 patients (with mostly stage II CRC) randomly assigned to fluorouracil and folinic acid or to observation (20% had central pathology review), there was a significant improvement in overall survival (risk reduction of 18% and 3·6% overall survival gain), with a similar benefit for colon and rectal cancers. This small benefit weighted against treatment toxicities and logistics, and co-morbidities, should be included in discussions of adjuvant chemotherapy. Tests of microsatellite instability might contribute to the risk benefit assessment of treatment in stage II disease. In QUASAR, patients with stage II CRC older than 70 years did not seem to benefit from chemotherapy, and the question is whether to treat or not to treat this age group. In the MOSAIC study, the benefit of adjuvant oxaliplatin and fluorouracil in stage II disease seemed small (no gain in 6-year overall survival, hazard ratio for 5-year disease-free survival 0·84), with a non-significant benefit in patients with high-risk stage II cancer (2·3% gain in 6-year overall survival, hazard ratio

for 5-year disease-free survival 0·72) (Andre *et al.,* 2009). Central to the decision-making process for adjuvant treatment (monotherapy or oxaliplatinbased) in all patients (stage II and III disease, older patients, and those with comorbidities) is discussion with the patient, and incorporation of the patient's preference after accurate communication of benefits and risks of treatment.

Of the targeted treatments assessed, addition of adjuvant edrecolomab (a monoclonal antibody against the epithelial cell adhesion molecule) and bevacizumab (a humanized monoclonal antibody against vascular endothelial factor [VEGF]) to chemotherapy did not improve disease-free survival (Fields *et al.,* 2009). Efficacy results from another study of adjuvant bevacizumab (AVANT study) are awaited, and an interim analysis of a randomized study of cetuximab (a monoclonal antibody targeted at the epidermal growth factor receptor [EGFR]) added to adjuvant fluorouracil and oxaliplatin has indicated a lack of benefit with the cetuximab combination. Disease relapse after surgery, with or without adjuvant chemotherapy, mostly occurs within 3 years. Intensive follow-up strategies for patients with colorectal cancer can improve survival, with the early detection of oligometastatic disease (commonly liver or lung) and potential for further radical treatment in a third of patients (Renehan *et al.,* 2002; Jeffery *et al.,* 2002; Tsikitis *et al.,* 2009). 5-year survival after liver and lung resection is about 36-58% and 27-41%, respectively (Jeffery *et al.,* 2002; Tsikitis *et al.,* 2009). Surveillance should be through a combination of clinical review, monitoring of serum carcinoembryonic antigen every 3-6 months for 3 years and then every 6-12 months until 5 years, imaging (most commonly CT) once a year for the first 3 years, and colonoscopy 1 year after surgery and then every 3-5 years (Tsikitis *et al.,* 2009; Chau *et al.,* 2004; Van *et al.,* 2009).

2.2.8 Problem of Therapy

2.2.8.1 Chemotherapy and Radiation

Fatigue, Hair loss, loss of appetite, mouth sores, nausea, vomiting, diarrhea and skin changes.

2.2.8.2Side Effects

Diarrhea, mucositis, skin effects, gastrointestinal toxicity, hematological toxicity, hearing damage and neurotoxicity.

2.2.8.3 Others

Higher costs, limited availability in some areas, difficulties associated with the administration (slow infusions) and prolonged duration of therapy.

2.2.9 Possible solution

Heading towards more effective and shorter course of treatment regimen with

- No side effects
- Economical
- Better activity
- Easily available
- Minimization of poisoning of healthy tissues
- Favourable Pharmacokinetic profile
- Better efficacy and safety profile

By the use of new drug molecules or by the use of new delivery systems of existing drugs.

2.3 Natural chemotherapeutic agents

2.3.1 Curcumin

Curcumin, commonly called diferuloyl methane, is a hydrophobic polyphenol derived from the rhizome (turmeric) of the herb *Curcuma longa*. Turmeric has been used traditionally for many ailments because of its wide spectrum of pharmacological activities. Curcumin has been identified as the active principle of turmeric; chemically, it is a bis-α, β-unsaturated β-diketone that exhibits keto-enol tautomerism. Curcumin has been shown to exhibit antioxidant, anti-inflammatory, antimicrobial, and anticarcinogenic activities (Kuttan *et al.,* 1985; Reddy *et al.,* 2005; Srimal & Dhawan, 1973). It also has

hepatoprotective and nephroprotective activities, suppresses thrombosis, protects against myocardial infarction, and has hypoglycemic and antirheumatic properties. Moreover, curcumin has been shown in various animal models and human studies to be extremely safe even at very high doses (Aggarwal *et al.,* 2003; Jagetia & Aggarwal, 2007; Aggarwal *et al.,* 2007; Shishodia *et al.,* 2007; Goel *et al.,* 2008; Anand *et al.,* 2007; Kunnumakkara *et al.,* 2008). Due to its pharmacological efficacy and safety, curcumin has been investigated in a wide range of research area *in-vitro* and *in-vivo*, in animal and human studies.

In spite of its various pharmacological activities and high safety, poor oral bioavailability can be one of the limiting factors in the clinical development of curcumin. The main reasons for low bioavailability of curcumin are its extremely low solubility in water, acidic and physiological pH, and its rapid hydrolysis under alkaline conditions (Tønnesen & Karlsen, 1985). The aqueous solubility of curcumin can be improved by increasing the pH of the solution. However, this approach leads to an undesirable outcome: a high rate of degradation by alkaline hydrolysis (Wang *et al.,* 1997).

2.3.2 Naringenin

Naringenin, a natural flavonoid aglycone of naringin, is widely distributed in citrus fruits (Dembinski *et al.,* 2004), tomatoes (Le Gall *et al.,* 2003), cherries (Wang *et al.,* 1999), grapefruit (Erlund *et al.,* 2001), and cocoa (Stark *et al.,* 2005). As a well-known antioxidant compound, the bioactivity of naringenin has been attributed to its structure-activity relationship. The number of hydroxyl substitutions of naringenin can donate hydrogen to ROS, allowing acquisition of stable structure, thus enabling scavenging of these free radicals (Shen *et al.,* 2004; Heo *et al.,* 2004). In addition, naringenin has also been extensively investigated for its pharmacological activities, including antitumor (Kanno *et al.,* 2005), anti-inflammatory (Hirai *et al.,* 2007), and hepatoprotective (Lee *et al.,* 2004) effects. Although naringenin possesses excellent free radical scavenging ability and pharmacological activities, clinical studies exploring different

schedules of administration of this drug have been hampered by its extreme water insolubility. It has also been reported that the absolute bioavailability of naringenin only achieved 4% in rabbits when the animals were orally administered (Hsiu *et al.,* 2002).

2.4 Influence of curcumin and naringenin on the carcinogenesis stages: Cell cycle and apoptosis

2.4.1 Inhibition of cell proliferation

Curcumin and naringenin has been shown to inhibit the proliferation of numerous cancer cell lines by causing arrest in G1/M phase (Hchen *et al.,* 1999; Saija *et al.,* 1995). By suppressing ornithine decarboxylase (ODC) activity, curcumin and naringenin has been shown to inhibit proliferation of breast cancer cells and also induce their arrest in the G1/S phase (Simon *et al.,* 1998). Cyclin D1 is necessary for cells to progress through the G1 phase of the cell cycle. Cyclin D1 gene expression is down regulated by curcumin and naringenin via decreased activation of nuclear factor-κB (NF-κB) (Shishodia *et al.,* 2005; Bharti *et al.,* 2003).

Additionally, from the point of view of cancer angiogenesis, it is important to note that curcumin and naringenin arrests the proliferation of human vascular endothelial cells (HUVEC) cells by accumulating them in the S phase (Singh *et al.,* 1996). It is important to note that as curcumin and naringenin causes cell cycle arrest in the G2/M phase, it raises the possibility whether curcumin and naringenin could render the cells sensitive to radiation and thus could be a potential radiosensitizer (Hchen *et al.,* 1999; Khafif *et al.,* 2005).

2.4.2 Proapoptotic property

Curcumin and naringenin induces apoptosis in various transformed cells in vitro including immortalized NIH3T3 fibroblasts and CRC cells (Scott & Loo, 2004). Moreover, it has been shown to induce apoptosis of cancer cells without

any significant cytotoxic effects on healthy cells (Aggarwal *et al.,* 2006). Some of the proapoptotic mechanisms include generation of reactive oxygen species, induction of p53 and proapoptotic proteins such as BAX while down regulating antiapoptotic genes Bcl-2 and BclXL (Tsvetkov *et al.,* 2005). Curcumin and naringenin stimulates the release of cytochrome c from mitochondria leading to caspase 3 activation, which results in cleavage of polyadenosine ribose polymerase (PARP) and inhibitor of caspase activated deoxyribonuclease (ICAD) (Han *et al.,* 1999). Loss of growth promoting signals via inhibition of transcription factors NF-κB, activating protein-1 (AP-1), and c-JUN and downregulation of proto-oncogenes Erg1 and c-MYC play a significant role in curcumin and naringenin induced apoptosis (Han *et al.,* 1999). Thus, curcumin and naringenin induced apoptosis can be mediated by both mitochondria dependent and independent mechanisms.

2.4.3 Inhibition of angiogenesis

Curcumin and naringenin inhibits proliferation of HUVEC and HVSMC cells at micromolar concentrations, resulting in inhibition of vascular tubule formation (Singh *et al.,* 1996). This is mediated in part by down regulation of proangiogenic factors such as VEGF and angiopoetin 1 and 2 (Gururaj *et al.,* 2002). It has also been shown to inhibit platelet derived growth factor (PDGF) induced proliferation of vascular smooth muscle cells (VSMC) *in-vitro* (Yang *et al.,* 2006).

2.4.4 Inhibition of carcinogenesis

Carcinogens are hydrocarbon compounds that are activated by cytochrome p-450 (CYP450) enzymes upon entering the body. Curcumin and naringenin inhibits the activity of CYP450 as demonstrated by a decrease in the alkylation of ethoxyresorufin in rat liver and decrease in aflatoxin induced DNA adduct formation, processes that require the CYP450 system (Thapliyal & Maru, 2001). DMBA, like other hydrocarbon carcinogens, binds to the Aryl

Hydrocarbon receptor (AhR); and this dimer binds to the response element (RE) on the promoter region of the CYP gene, thus increasing its transcription (Rinaldi *et al.,* 2002). Curcumin and naringenin binds to AhR, thus preventing it from binding to the RE of the CYP gene (Rinaldi *et al.,* 2002).

The effect of curcumin and naringenin on Phase 2 reactions is concentration dependent, activating glutathione transferase (GST) at low doses and inhibiting at high doses (Sharma *et al.,* 2001). Curcumin's as well as naringenin's effect on GST also depends on the presence of carcinogens. It has been shown to inhibit GST in cells treated with carcinogens and activates it in normal cells (Sharma *et al.,* 2001). Overall, the data support inhibition of carcinogenesis by curcumin and naringenin at initiation phase by inhibiting activation of carcinogens through CYP450 enzymes and increasing clearance by making them water soluble.

2.4.5 Inhibition of COX-2

Curcumin and naringenin is a potent inhibitor of COX-2. This action on COX-2 is most likely mediated by NF-κB down regulation, which is one of the major inducers of COX-2 promoter activation (Plummer *et al.,* 1999). Celecoxib and curcumin/naringenin, when administered together, synergistically inhibit human CRC cells (Lev-Ari *et al.,* 2005). Four different cell lines of human CRC, namely, HT29, IEC-18-Kras, Caco-2, and SW-480, were treated with celecoxib, curcumin/naringenin or both. It was demonstrated that the combination of celecoxib and curcumin/naringenin synergistically inhibited proliferation and induced apoptosis by down regulating COX-2 expression (Lev-Ari *et al.,* 2005).

2.4.6 Down regulation of EGFR and human epidermal growth factor receptor 2 (HER2)/neu mediated signal transduction

EGFR family of proto-oncogenes encodes tyrosine kinases, which are down regulated by curcumin and naringenin to inhibit growth in neoplastic cells.

Curcumin and naringenin has been shown to down regulate both intrinsic tyrosine kinase activity of EGFR as well as EGF mediated phosphorylation of the receptor (Korutla & Kumar, 2004; Korutla *et al.,* 1995). HER2/neu tyrosine kinase activity is also decreased upon treatment with curcumin and naringenin (Leu *et al.,* 2002). Moreover, curcumin and naringenin induces intracellular degradation of HER2/neu like geldanamycin (Tikhomirov *et al.,* 2003). Curcumin and naringenin also leads to the decreased levels of total EGFR and HER2 through inhibition of promoter transcriptional activity and by dissociating its binding to the chaperone molecule (GRP94), respectively (Chen *et al.,* 2006).

Curcumin and naringenin increases the gene expression of and activates the nuclear hormone receptor PPAR-γ in hepatic satellite cells. PPAR-γ antagonists reduce the ability of curcumin and naringenin to inhibit cell proliferation (Chen & Xu, 2005). In Moser cells, the activation of PPARγ by curcumin leads to down regulation of cyclin D1 and EGFR gene expression (Xu *et al.,* 2003).

2.4.7 Down regulation transcription factor NF-κB

NF-*κ*B is a nuclear transcription factor for genes encoding inflammatory cytokines, major histocompatibility complex (MHC) genes, adhesion molecules, COX2 and genes responsible for resistance to chemotherapy. Curcumin and naringenin inhibits both constitutive and H_2O_2, tumor necrosis factor (TNF) and phorbol acetate induce NF-*κ*B activation (Singh & Aggarwal, 1995). Curcumin and naringenin inhibits NF-*κ*B activity via blocking NF-*κ*B from binding to DNA and IKK complex activation, which blocks I*κ*-*βα* phosphorylation (Jobin *et al.,* 1999; Plummer *et al.,* 1999). This leads to down regulation of NF-*κ*B mediated gene expression of adhesion molecules intracellular adhesion molecule-1 (ICAM-1), vascular cell adhesion molecule-1 (VCAM-1), and endothelial leukocyte adhesion molecule-1 (ELAM-1), thus suppressing tumor metastasis (Kumar *et al.,* 1998).

In addition, matrix metalloprotein-9 (MMP-9) is down regulated by curcumin as well as naringenin again via down regulation of NF-κB (Shishodia *et al.,* 2003; Aggarwal *et al.,* 2005). Matrix metalloproteinase are proteases that contribute to metastasis, and thus MMP-9 down regulation contributes to curcumin and naringenin mediated inhibition of metastasis.

Telomerase is an enzyme that splits the telomeres located at chromosomal terminals at the end of each cell division, thus restricting the total number of cell divisions that the cell can undergo. Telomerase activity is decreased in many cancers. Curcumin and naringenin treated breast cancer cells showed a marked inhibition of telomerase activity (Ramachandran *et al.,* 2002). This inhibition was due to a decrease in hTERT expression, probably mediated by NF-κB inhibition. Inhibition of telomerase by curcumin and naringenin has been demonstrated in other cancer cell lines as well (Mukherjee *et al.,* 2007; Chakraborty *et al.,* 2006). Thus, attenuation of NF-κB activity is considered central to many of curcumin's as well as narinegnin's anticancer properties.

2.4.8 Inhibition of AP-1

AP-1 is a transcription factor that regulates genes involved in carcinogenesis, cell proliferation, and progression of benign tumors to malignancy and in metastasis. It is formed by dimerization of activated c-Jun, and c-FOS (Karin *et al.,* 1997). Curcumin and naringenin inhibits c-Jun N terminal kinase activation by carcinogens, thus inhibiting c-Jun phosphorylation and consequently AP-1 activation (Xia *et al.,* 2000; Chen & Tan, 1998). Curcumin and naringenin has also been shown to down regulate tumor promoting agent (TPA) induced activation of both c-Jun and c-FOS (Kakar & Roy, 1994). Further, by directly interacting with the DNA binding motif of AP-1, curcumin prevents its actions on gene expression (Bierhaus *et al.,* 1997).

2.5 Literature review related to curcumin and naringenin formulations

The curcumin and naringenin formulations and its related literature search are as follows:

Table 2.1 List of curcumin and naringenin formulations

S. No.	Title	Reference
1.	Preparation and characterization of water-soluble albumin-bound curcumin nanoparticles with improved antitumor activity	Kim *et al.,* 2011
2.	Evaluation of novel alginate foams as drug delivery systems in antimicrobial photodynamic therapy (aPDT) of infected wounds-an in vitro study: studies on curcumin and curcuminoides XL	Hegge *et al.,* 2010
3.	Novel artemisinin and curcumin micellar formulations: drug solubility studies by NMR spectroscopy	Lapenna *et al.,* 2008
4.	Characterization of curcumin–PVP solid dispersion obtained by spray drying	Paradkar *et al.,* 2004
5.	Controlled release of oral tetrahydrocurcumin from a novel self-emulsifying floating drug delivery system (SEFDDS)	Setthacheewakul *et al.,* 2011
6.	Curcumin enhances oral bioavailability and anti-tumor therapeutic efficacy of paclitaxel upon administration in nanoemulsion formulation	Ganta *et al.,* 2010
7.	Curcumin-loaded hydrogel nanoparticles: Application in anti-malarial therapy and toxicological evaluation	Dandekar *et al.,* 2010
8.	Bioavailability enhancement of curcumin by complexation with phosphatidylcholine	Gupta *et al.,* 2011
9.	Preparation and pharmacokinetic evaluation of curcumin solid dispersion using Solutol® HS15 as a carrier	Seo *et al.,* 2012
10.	Improved bioavailability of poorly water-soluble drug curcumin in cellulose acetate solid dispersion	Wan *et al.,* 2012
11.	Curcumin-phospholipid complex: Preparation, therapeutic evaluation and pharmacokinetic study in rats	Maiti *et al.,* 2007
12.	Optimization and formulation design of gels of diclofenac and curcumin for transdermal drug delivery	Chaudhary *et al.,* 2011

	by box-behnken statistical design	
13.	Encapsulation of curcumin by methoxy poly(ethylene glycol-b-aromatic anhydride) micelles	Hong *et al.,* 2011
14.	Formulation and characterization of curcuminoids loaded solid lipid nanoparticles	Tiyaboonchai *et al.,* 2007
15.	High-performance liquid chromatography analysis of curcumin in rat plasma: application to pharmacokinetics of polymeric micellar formulation of curcumin	Ma *et al.,* 2007
16.	Synthesis and characterization of hydrogel-silver nanoparticle-curcumin composites for wound dressing and antibacterial application	Varaprasad *et al.,* 2011
17.	Effect of curcumin on liposome: curcumin as a molecular probe for monitoring interaction of ionic liquids with 1,2-Dipalmitoyl-sn-Glycero-3-Phosphocholine liposome	Patra *et al.,* 2012
18.	Loading of curcumin into macrophages using lipid-based nanoparticles	Sou *et al.,* 2008
19.	Liposomal delivery system enhances anti-inflammatory properties of curcumin	Basnet *et al.,* 2012
20.	Effects of different carboxylic ester spacers on chemical stability, release characteristics, and anticancer activity of mono-PEGylated curcumin conjugates	Wichitnithad *et al.,* 2011
21.	In-situ injectable nano-composite hydrogel composed of curcumin, N,O-carboxymethyl chitosan and oxidized alginate for wound healing application	Li *et al.,* 2012
22.	Formulation design and photochemical studies on nanocrystal solid dispersion of curcumin with improved oral bioavailability	Onoue *et al.,* 2010
23.	Enhancement of oral absorption of curcumin by self-microemulsifying drug delivery systems	Cui *et al.,* 2009
24.	Novel lipid based oral formulation of curcumin: Development and optimization by design of	Pawar *et al.,* 2012

	experiments approach	
25.	Physicochemical characterization of curcuminoid-loaded solid lipid nanoparticles	Noack *et al.,* 2012
26.	Poly(b-cyclodextrin)/Curcumin self-assembly: A novel approach to improve curcumin delivery and its therapeutic efficacy in prostate cancer cells	Yallapu *et al.,* 2010
27.	Synthesis and characterization of a cytotoxic cationic polyvinylpyrrolidone–curcumin conjugate	Manju & Sreenivasan, *et al.,* 2011
28.	Exploring solid lipid nanoparticles to enhance the oral bioavailability of curcumin	Kakkar *et al.,* 2011
29.	Highly loaded, sustained-release microparticles of curcumin for chemoprevention	Shahani & Panyam *et al.,* 2011
30.	Formulation, characterization and evaluation of curcumin-loaded PLGA nanospheres for cancer therapy	Mukerjee & Vishwanatha *et al.,* 2009
31.	Injectable sustained release microparticles of curcumin: A new concept for cancer chemoprevention	Shahani *et al.,* 2010
32.	The in vitro stability and in vivo pharmacokinetics of curcumin prepared as an aqueous nanoparticulate formulation	Mohanty & Sahoo, 2010
33.	Beta casein-micelle as a nano vehicle for solubility enhancement of curcumin; food industry application	Esmaili *et al.,* 2011
34.	Characterization of curcuemulsomes: nanoformulation for enhanced solubility and delivery of curcumin	Ucisik *et al.,* 2013
35.	Oral delivery of curcumin bound to chitosan nanoparticles cured *Plasmodium yoelii* infected mice	Akhtar *et al.,* 2012
36.	Controlled systemic delivery by polymeric implants enhances tissue and plasma curcumin levels compared with oral administration	Bansal *et al.,* 2012
37.	Synthesis and in vitro/in vivo anti-cancer evaluation of curcumin-loaded chitosan/poly(butyl cyanoacrylate) nanoparticles	Duan *et al.,* 2010

38.	In vivo evaluation of curcumin nanoformulation loaded methoxy poly(ethylene glycol)-graft-chitosan composite film for wound healing application	Li *et al.,* 2012
39.	Curcumin nanodisks: formulation and characterization	Ghosh *et al.,* 2011
40.	Enhancing anti-inflammation activity of curcumin through O/W nanoemulsions	Wang *et al.,* 2008
41.	Curcumin-phospholipid complex: Preparation, therapeutic evaluation and pharmacokinetic study in rats	Maiti *et al.,* 2007
42.	Cyclodextrin-complexed curcumin exhibits anti-inflammatory and antiproliferative activities superior to those of curcumin through higher cellular uptake	Yadav *et al.,* 2010
43.	Encapsulation of curcumin in alginate-chitosan-pluronic composite nanoparticles for delivery to cancer cells	Das *et al.,* 2010
44.	Enhancement of oral absorption of curcumin by self-microemulsifying drug delivery systems	Cui *et al.,* 2009
45.	Water-dispersible multifunctional hybrid nanogels for combined curcumin and photothermal therapy	Wu *et al.,* 2011
46.	Nanoparticle encapsulation improves oral bioavailability of curcumin by at least 9-fold when compared to curcumin administered with piperine as absorption enhancer	Shaikh *et al.,* 2009
47.	An *in vitro* study of liposomal curcumin: Stability, toxicity and biological activity in human lymphocytes and Epstein-Barr virus-transformed human B-cells	Chen *et al.,* 2009
48.	Nanoemulsion- and emulsion-based delivery systems for curcumin: Encapsulation and release properties	Ahmed *et al.,* 2012
49.	Purely aqueous PLGA nanoparticulate formulations of curcumin exhibit enhanced anticancer activity with dependence on the combination of the carrier	Nair *et al.,* 2012
50.	Optimised nano-formulation on the bioavailability of hydrophobic polyphenol, curcumin, in freely-moving	Tsai *et al.,* 2011

	rats	
51.	Polymeric micelles for parenteral delivery of curcumin: Preparation, characterization and in vitro evaluation	Song *et al.,* 2011
52.	Polymeric nanoparticle-encapsulated curcumin ("nanocurcumin"): a novel strategy for human cancer therapy	Bisht *et al.,* 2007
53.	Release characteristic and stability of curcumin incorporated in β-chitin non-woven fibrous sheet using Tween 20 as an emulsifier	Ratanajiajaroen *et al.,* 2012
54.	Development and evaluation of self-microemulsifying liquid and pellet formulations of curcumin, and absorption studies in rats	Setthacheewakul *et al.,* 2010
55.	Safety assessment of a solid lipid curcumin particle preparation: Acute and subchronic toxicity studies	Dadhaniya *et al.,* 2011
56.	Efficient water soluble O-carboxymethyl chitosan nanocarrier for the delivery of curcumin to cancer cells	Anitha *et al.,* 2011
57.	Water-dispersible multifunctional hybrid nanogels for combined curcumin and photothermal therapy	Wu *et al.,* 2011
58.	Encapsulation of curcumin in self-assembling peptide hydrogels as injectable drug delivery vehicles	Altunbas *et al.,* 2011
59.	Evaluation of nanotechnology-based carrier for delivery of curcumin in prostate cancer cells	Thangapazham *et al.,* 2008
60.	Evaluating potential of curcumin loaded solid lipid nanoparticles in aluminium induced behavioural, biochemical and histopathological alterations in mice brain	Kakkar & Kaur, 2011
61.	Development and in vitro in vivo evaluation of polymeric implants for continuous systemic delivery of curcumin	Bansal *et al.,* 2011
62.	Naringin and naringenin determination and control in grapefruit juice by a validated HPLC method	Ribeiro & Ribeiro, 2008
63.	Anomalous dissolution property enhancement of naringenin from spray-dried particles with α-	Tozuka *et al.,* 2010

	glucosylhesperidin	
64.	Combined effect of pH and polysorbates with cyclodextrins on solubilization of naringenin	Tommasini *et al.,* 2004
65.	Naringenin-loaded nanoparticles improve the physicochemical properties and the hepatoprotective effects of naringenin in orally-administered rats with CCl_4-induced acute liver failure	Yen *et al.,* 2009
66.	Preparation and physicochemical properties of the complex of naringenin with hydroxypropyl-β-cyclodextrin	Wen *et al.,* 2010
67.	Characterize the interaction between naringenin and bovine serum albumin using spectroscopic approach	Hua *et al.,* 2010
68.	Preparation and characterization of inclusion complexes of naringenin with β-cyclodextrin or its derivative	Yang *et al.,* 2013
69.	Improvement in solubility and dissolution rate of flavonoids by complexation with β-cyclodextrin	Tommasini *et al.,* 2004
70.	Anomalous dissolution property enhancement of naringenin from spray-dried particles with α-glucosylhesperidin	Tozuka *et al.,* 2010
71.	Coimmobilization of naringinases on silk fibroin nanoparticles and Its application in food packaging	Wu *et al.,* 2013
72.	Enhancement of naringenin solution concentration by solid dispersion in cellulose derivative matrices	Li *et al.,* 2013
73.	Preparation and characterization of phospholipid complexes of naringenin for effective drug delivery	Semalty *et al.,* 2010
74.	Chemopreventive efficacy of naringenin-loaded nanoparticles in 7,12-dimethylbenz(a)anthracene induced experimental oral carcinogenesis	Sulfikkarali *et al.,* 2013
75.	Solubility of naringenin in ethanol and water mixtures	Zhang *et al.,* 2013

2.6 Nanotechnology based phyto-formulations

Nanoformulations of phyto compounds essentially follow the general principles of nanotechnology. Therefore, the nanotechnology platforms are widely being used create delivery systems for bioactive natural products and nutraceuticals with poor water solubility. The market projections for these technologies suggest a multifold increase in their commercial potential over the next 5 years. The novel carriers should ideally fulfill two prerequisites. Firstly, it should deliver the drug at a rate directed by the needs of the body, over the period of treatment. Secondly, it should channel the active entity of herbal drug to the site of action. Conventional dosage forms including prolonged-release dosage forms are unable to meet none of these.

According to the National Nanotechnology Initiative (NNI; http://www.nano.gov) nanotechnologic structures should be only 1-100 nm in at least one dimension. This size requirement can be achieved through various rational designs, including top-down and bottom-up approaches. Nanocarriers have the potential to modify modern drugs by increasing their efficacy, stability, and solubility, decreasing their toxicity, and sustaining their release (Merisko-Liversidge & Liversidge, 2008). Nanoparticulate drug delivery systems using polymeric nanoparticles, liposomes, nanocapsules, solid-lipid nanoparticles, phytosomes and nanoemulsion, etc have attracted increasing attention in recent years. The most noticeable nanotechnologic applications in medicine have been related to oncology (Mousa *et al.,* 2007; Davis *et al.,* 2008).

The term 'nanoncology' refers to the application of nanotechnologies to the cancer field for therapeutic, imaging as well as diagnostic purposes. The active agent is dissolved, entrapped, adsorbed, covalently attached or encapsulated in the nanocarrier giving an array of architectures and functionalities. In the case of conventional chemotherapeutics, this approach is considered beneficial in solving solubility issues and inconsistent bioavailability, based on the concept that pharmacokinetics of an anticancer drug can be usefully altered in the body to promote drug accumulation predominantly in pathological

sites (Jain, 2010; Wang & Thanou, 2010; Mattheolabakis *et al.,* 2012; Bourzac, 2012; Davis *et al.,* 2008). The therapeutic effects of some anticancer drugs could be significantly improved also if drug delivery occurs specifically to organelles inside cancer cells. Thus, an appropriate design allows nanoconstructs to improve drug efficacy (activity at lower doses) as compared with the free-drug treatment, giving in turn a wider therapeutic window and lower side effects. Furthermore, nanocarriers are also capable of addressing several drug delivery problems, which could not be effectively solved in the past. Overcoming multidrug resistance (MDR) phenomenon and penetrating cellular barriers that may limit device accessibility to intended targets, such as the blood-brain barrier, remain unsolved issues where nanodelivery technologies can play a key role. On the other hand, engineered nanocarriers have many potential benefits for diagnosing and treating metastatic cancer, including the ability to transport complex molecular cargo to the major sites of metastasis, such as lungs, liver and lymph nodes, as well as targeting to specific cell populations within these organs (Schroeder *et al.,* 2012). Another aspect covered by nanocarriers relies on the significant opportunity to apply nanotechnologies in molecular cancer imaging and diagnosis (Schroeder *et al.,* 2012; Mura & Couvreur, 2012; Huang *et al.,* 2011). Tumor imaging plays a central role in clinical oncology by helping: i) to identify solid tumors, ii) to determine recurrence and iii) to monitor therapeutic responses. Imaging techniques use different contrast agents, which, once engineered or incorporated in nanoparticles, can allow efficient single or multimodal imaging in cancer detection. Indeed, the main advantage of increased image resolution is discovering lesions so small to be undetectable with conventional techniques and also monitoring disease progression, which would represent a significant improvement over the available clinical diagnostic methods. Furthermore, nanoprobes, such as quantum dots (QDs), can be used to identify a panel of biomarkers on intact cancer cells and tissue specimens, thus allowing a deeper understanding of cancer behavior and early cancer detection (Nie *et al.,* 2007). Integration of an imaging element in a nano-construct makes it possible to follow biodistribution in the body in real time, which can be useful to optimize carrier design in order to reach a specific area in the body and to

elucidate toxicological concerns. Finally, imaging techniques and treatment strategies can be properly combined in the same entity giving rise to multifunctional theranostic nanomedicines conveying unique advantages for cancer treatment (Caldorera-Moore *et al.,* 2011; Janib *et al.,* 2010; Park *et al.,* 2009; Xie *et al.,* 2010). The behavior of nanocarriers in a living body and their interaction with biological environment is driven by physiochemical features of the nanocarrier such as size, shape, deformability, surface properties, stability, dose and route of administration, all of them considered crucial for a beneficial therapeutic outcome. Thus, a huge amount of nanosystems with more or less complicated design have been developed over the past few decades and there has been intense effort towards understanding how nanocarrier properties can be properly manipulated for oncology applications.

Nanocarrier size: The National Cancer Institute currently recommends that the size of the nanocarriers be 10-100 nm. Even though the upper limit of nanocarrier size is not strictly defined, the lower limit (10 nm) is fixed based on the threshold for first-pass elimination by the kidneys (Silva & da Boit, 2010). Size is a key factor in the biodistribution of long-circulating nanoparticles on the basis of physiological parameters such as hepatic filtration, tissue extravasation, tissue diffusion and kidney excretion (Alexis *et al.,* 2008). Tumor-targeting nanoparticles must resist hydrostatic and biophysical/biochemical barriers, overcome cellular resistance to treatment, resist biotransformation, and resist sudden degradation, immediate clearance, and enhanced distribution even in poorly perused areas (Jain, 1987).

Surface characteristics: The surface properties of nanocarriers determine their interaction with the local environment. Sterically stabilized nanocarriers exhibit minimal self and non-self interactions (Davis *et al.,* 2008). These particles keep slightly high or low negative or positive charges on their surface, which leads to an increased reticuloendothelial clearance; therefore, minimizing nonspecific interactions and controlling surface charge by steric stabilization helps to prevent nanocarrier loss in undesired locations to a certain extent. Nanocarriers have high surface-to-volume ratios, which can be manipulated by

rational design. The surface properties of the nanocarriers will determine their solubility, stability, and clearance. It has been shown that polymer drug or antibody conjugates have superior half-lives, which can improve the pharmacokinetics of the drug (Duncan *et al.,* 2005). Increased opsonization associated with nanocarriers surface during circulation can trigger substantial hepatic agglomeration.

2.7 Nanoparticulate targeting

Any ideal therapy to treat a disease should destroy specifically diseased or affected cells in an organ while conserving normal cells. Ultimately, targeting will enable the cancer cells to receive the pharmacologically required concentration of the drug molecules. Various targeting approaches, including passive and active targeting of drug molecules, are well characterized and studied. A large body of evidence suggests that these targeting strategies could overcome drug resistance and side effects to the vital organs and could minimize systemic drug administration.

2.7.1 Passive Targeting and its application

Passive targeting takes advantage of the unique properties of tumor vasculature and microenvironment (Maeda *et al.,* 2000). In fact, architectural defectiveness and high degree of vascular density generate abnormal tumor vessels, aberrant branching and blind loops of twisted shape as depicted in Figure 2.2. Blood flow behavior, such as direction of blood flow, is also irregular or inconsistent in these vessels. When compared with normal vessels, tumor vessels are 'leaky,' owing to basement membrane abnormalities and a decreased number of pericytes lining the rapidly proliferating endothelial cells. The pore size of tumor vessels varies from 100 nm to almost 1 mm in diameter, depending upon the anatomic location of the tumors and the stage of tumor growth. Moreover, as the functionality of tumor lymphatic vessels is generally poor, solid tumors are characterized by decreased clearance of macromolecules and their consequent retention in tumor interstitium. The unique pathophysiologic characteristics of tumor vessels coupled with poor lymphatic drainage induce

the EPR effect, which enables macromolecules to extravasate through these gaps into extravascular spaces and accumulate inside tumor tissues. After pioneering results (Matsumura & Maeda *et al.,* 1986), researchers have capitalized this concept for the delivery of various drugs by either building drug-polymer conjugates or encapsulating drugs within nanocarriers.

Nowadays, it is evident that long-circulating nanosized carriers accumulate passively in tumors due to the EPR effect (Duncan, 2003) and the vast majority of nanomedicines developed for drug targeting to tumors rely on this effect. After approval of liposomal doxorubicin (Doxil), Abraxane and Genexol-PM have followed as first examples of marketed products based on polymeric nanocarriers. Several additional passively tumor-targeted nanomedicines are currently in clinical trials, and a large number of other ones are in early and late-stage pre-clinical development. Nevertheless, exploiting EPR effect to deliver a drug to a solid tumor is a complicated matter (Fang *et al.,* 2011; Maeda, 2012). The journey of nanocarriers in the body has been recently reviewed (Bertrand & Leroux, 2012). Natural elimination processes, including both renal clearance and mononuclear phagocyte system (MPS) uptake, play a pivotal role in driving nanocarrier circulation in the body. Filtration of particles through the glomerular capillary wall is highly dependent on molecule size and is referred to as the filtration-size threshold. Molecules with a diameter of <5 nm are typically filtered, while those with a size >8 nm are not typically capable of glomerular filtration.

The uptake of nanocarriers in MPS, also referred to as the reticuloendothelial system (RES), proceeds quickly and must be avoided in order to have an acceptable circulation time MPS, is the main natural clearance system for particles not filtered by the kidneys acting via phagocytosis. Recognition by the MPS is aided by opsonisation, which induces nanosystem phagocytosis and accumulation in the liver. Protein adsorption is driven by nanocarrier properties and has been considered a key factor to control nanocarrier biological behaviour ab initio (Monopoli *et al.,* 2012; Karmali & Simberg, 2011). Several tools are available to exactly identify composition of bound protein cloud (Lundqvist *et al.,*

2008). The liver acts as a reservoir toward nanocarriers, conditioning their rapid first-phase disappearance from the blood and, in case of biodegradable systems, their second-phase release in the body under degraded and excretable form. This biodistribution can be of benefit for the chemotherapeutic treatment of MPS-localised tumors (e.g., hepatocarcinoma or hepatic metastasis arising from digestive tract or gynaecological cancers, bronchopulmonary tumors, myeloma and leukaemia). Ideally, an injectable nanocarrier has to be small enough to avoid internalisation by the MPS but large enough to avoid renal clearance (100-200 nm). Recent finding highlight that variation of nanocarrier dimension in the scale length >100 nm can heavily affect blood circulation time as in the case of filo micelles (Geng *et al.,* 2007), whereas the role of geometry in driving in-vivo biodistribution has not been clarified yet (Euliss *et al.,* 2006; Decuzzi *et al.,* 2009).

In order to overcome the opsonisation of nanocarriers, a number of strategies have been investigated to make them 'invisible' to the immune system, creating long-circulating nanocarriers, known also as 'stealth' systems. Hydrophilic polymers can form a cloud on nanocarrier surface, which repels opsonins and possibly adsorbs disopsonins giving decreased levels of uptake by the MPS and increased circulation time in the blood (Owens & Peppas, 2006). To disclose the mechanistic action of hydrophilic clouds around nanocarrier and manipulate its PK through rational design, relevant literature has been produced in the last few years (Moghimi *et al.,* 2012). Longevity in the blood can promote nanocarrier accumulation in solid tumors passing through their leaky vasculature (passive targeting). Particles with hydrophobic surfaces, in fact, will preferentially be taken up by the liver, followed by the spleen and lungs, while particles with long circulation times should be 100 nm or less in diameter and have a hydrophilic surface in order to reduce clearance by macrophages (Alexis *et al.,* 2008). As a result, non-targeted nanocarriers accumulate in tumors of xenograft mice models in the range 1-4% of the injected dose/g of tissue although these numbers are difficult to derive due to different post-injection

time assessments and tumor type (Alexis *et al.,* 2008). Furthermore, it is not clear whether circulation half-life or maximum tolerated dose is the most critical parameter for optimal accumulation in tumor tissue of a given drug (Alexis *et al.,* 2010).

In the case of humans, it is very hard to compare PK of different systems due to inter variability as well as cancer staging. Furthermore, a steric stabilization of nanocarrier surface limits also aggregation between particles themselves in the blood and contributes to system stability in biological environments. Nanocarriers prepared from poly(ethylene glycol) (PEG)-modified polymers are certainly the most explored systems for intravenous cancer therapy. PEGylation facilitates MPS escape, significantly increases blood circulation time and benefits EPR-based targeting of drugs to tumors (Gref *et al.,* 2012). Besides hydrophilicity and surface density, chain flexibility is a major feature to provide prolonged drug circulation since PEG cloud should in theory prevent immune system from modeling an antibody against it. However, it has been recently demonstrated that PEGylated nanoparticles and micelles can lose their long-circulating characteristics when administered within a certain time interval from injection of the first dose, in the same animal the so-called accelerated blood clearance (ABC) phenomenon (Ishida & Kiwada, 2008). This effect has been attributed to the fact that PEG in itself may be immunogenic and that the induced anti-PEG antibodies are linked to enhanced blood clearance, accumulation in the liver and reduced efficacy of the products. This unexpected phenomenon, being a potential challenge for PEGylated nanocarrier applications, would greatly compromise the benefits of nanocarrier use for cancer diagnosis and therapy and will be worth of further investigation in the next future.

In fact, the induction of the ABC phenomenon seems to be a complicated process. The following mechanism was very recently set to explain it: once PEGylated nanocarriers (first dose) reach the spleen, they bind and cross-link to surface immunoglobulins on reactive B cells in the splenic marginal zone and

consequently triggers the production of anti-PEG IgM. Upon administration of the second or subsequent dose, if anti-PEG IgM still exists in the blood circulation, it binds to surface PEG, and subsequently activates the complement system, resulting in opsonisation by C3 fragments and enhanced uptake by Kupffer cells via complement receptor-mediated endocytosis (bu Lila *et al.,* 2013). Nevertheless, as underlined by the authors themselves, this mechanism can only partly explain ABC, which could not be totally reversed upon spleen removal, suggesting that other factors/tissues are involved.

Of note is the recent finding of a 22-25% occurrence of anti-PEG IgM in healthy blood donors, which is a very high value if compared with the 0.2% occurrence reported 20 years ago (Garay *et al.,* 2012). The authors attributed this phenomenon to an improvement of the limit of detection of antibodies during the years as well as to greater exposure to PEG-containing cosmetic, pharmaceutical and processed food products. Nevertheless, it has been also highlighted that several literature indications derive from assays for anti-PEG antibodies that are flawed and lack specificity (Schellekens *et al.,* 2013). Also the biological effects induced by anti-PEG IgM antibodies lack the characteristics of a bona fide antibody reaction, which is a point that will require other research efforts (Schellekens *et al.,* 2013). A paradigm shift in cancer therapy resides in precise control over the exposure of tumor-associated cells to anti-cancer drugs, which can result in therapeutic outcome by regimens that control drug levels, dosing intervals and drug retention in tumor. Thus, strategies allowing the exposure of cells to metered dose of an anti-cancer drug over longer periods can act more effectively than the same dose as a bolus (metronomic approach) (Pasquier *et al.,* 2010). Through exerting direct and indirect effects on tumor cells and their microenvironment, metronomic scheduling can inhibit tumor angiogenesis, stimulate anti-cancer immune response and directly affect tumor cell growth.

To this purpose, nano platforms with a sustained drug release may be highly beneficial in cancer treatment. Nevertheless, certain PEG-modified particles are also now understood to have a slower uptake into tumor cells than non-PEGylated molecules, thus generating drug gradients in the extracellular space of tumor site reaching further hypoxic regions. To do this, the release rate of the drug from the carrier at the target must be optimal (e.g. 3-10%/day), because a too slow release results in insufficient concentrations of active drugs at sites of action. Release that is too rapid would lead to a high concentration of free drug in circulation but no drug accumulation in the tumor, the results thus being a considerably lower therapeutic effect and undesired systemic toxicity.

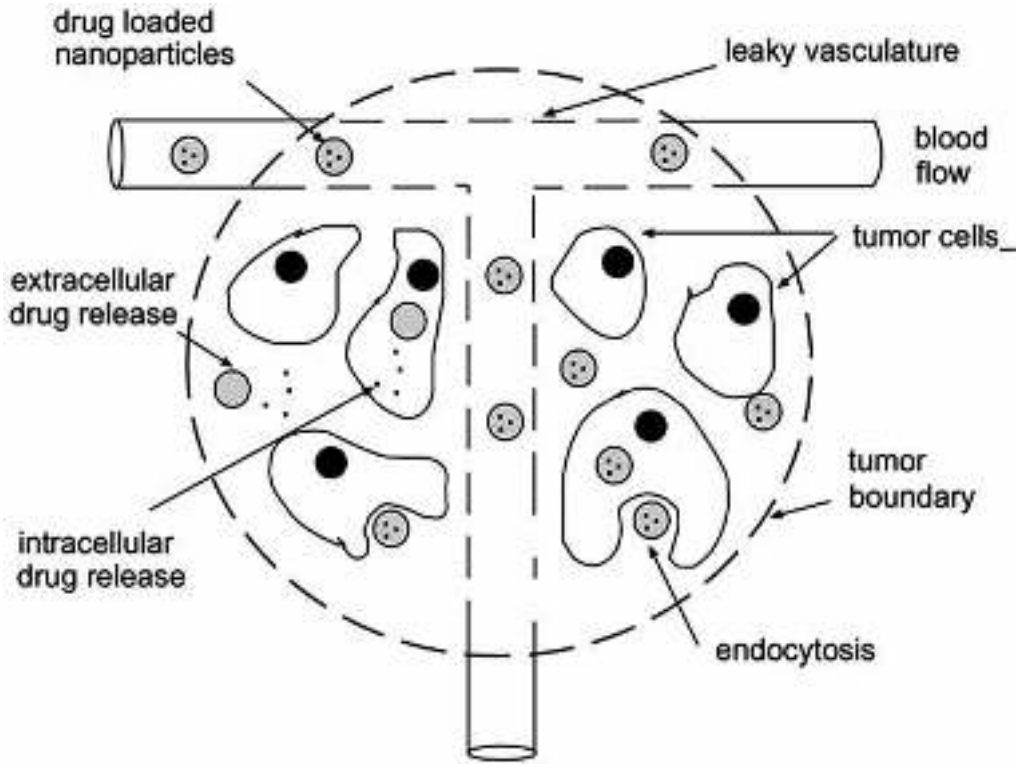

Figure 2.2 Passive targeting, the EPR effect; (Tumor tissues are known to have leaky vasculature and results in a passive accumulation of nanoparticles and this phenomenon is referred to as EPR) (Adapted from De Oliveira *et al.,* 2013).

2.7.2 Active targeting and its application

Targeting cancer cells through EPR effect is not feasible in all tumors because the degree of tumor vascularisation and porosity of tumor vessels can vary with the tumor type and status (Denison & Bae, 2012). A positive correlation clearly exists between tumor growth rate and the EPR effect, rendering the clinical significance of vascular permeability effect in drug delivery much debated. Little is known about the actual effectiveness of the EPR effect in metastatic or microscopic residual tumors at late stage of development, where targeted chemotherapy is most desired. To improve drug accumulation at tumor/cancer cell level, different approaches can be followed. By simply changing surface properties (charge, shielding cloud), one can manipulate nanocarrier interaction with cell membrane (Li *et al.,* 2012). Nevertheless, decoration of nanocarriers with different functional motifs is the approach most represented in the literature to build up actively targeted nano-constructs (Lammers *et al.,* 2008; Kamaly *et al.,* 2012). Surface exposure of a ligand recognizing a receptor over-expressed in cancer cells (folate, transferrin, prostate specific membrane antigen-interacting peptides or aptamers) is expected to increase drug amount inside cancer cells by activating receptor-mediated transport mechanisms (Danhier *et al.,* 2010) (Figure 2.3). Another approach resides in the decoration of nanocarrier surface with targeting moieties able to recognize tumor microenvironment (surface receptor on tumor blood vessels, as in the case of RGD peptides or extracellular matrix) (Danhier *et al.,* 2010). Many active targeting strategies have been developed, but despite this truly remarkable potential in applications, they have met with mixed success to date and the reasons for that are nowadays deeply discussed (Florence, 2012; Florence, 2012; Ruenraroengsak *et al.,* 2010; Lammers *et al.,* 2012; Kwon *et al.,* 2012; Bae & Park, 2011).

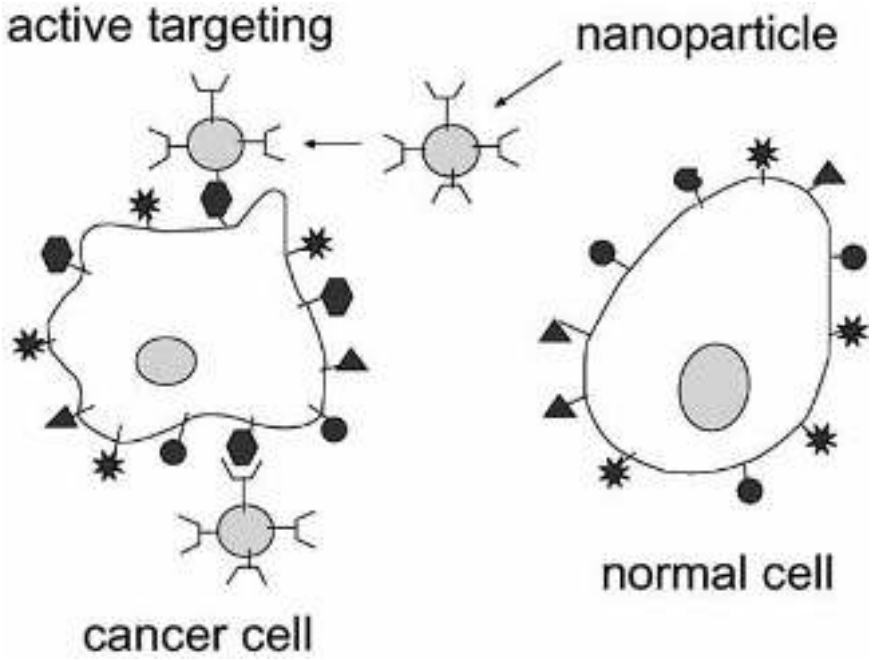

Figure 2.3 Active targeting: Nanoparticles with ligands or molecules attached to their surface can target tumor cells preferentially over healthy cells; (Adapted from de Oliveira *et al.,* 2013).

An important drawback of targeted nanocarriers is that they can paradoxically lose targeting ability in a biological environment. First, interaction with other proteins in the medium and the formation of a 'protein corona' can screen the targeting molecules on the surface of nanocarriers and cause loss of specificity in targeting (Salvati *et al.,* 2013). Another potential challenge related to molecular targeting is the so-called 'binding-site barrier' effect, which may confine the drug in the perivascular regions retarding drug/nanocarrier tumor penetration (Lee *et al.,* 2010). This effect is mainly dictated by particle size and ligand-receptor affinity. In fact, the diffusion of extravasated nanocarriers from the perivascular into the a vascular region will be inversely correlated with their molecular size, which increases upon exposure of surface ligands. On the other hand, when a high-affinity ligand diffuses into the tumor, the slow off rate mediated by its long association may preclude the docking of other ligands to the same receptor, impeding them from traversing tumors using sequential binding to and dissociation from unoccupied receptors (Baxter & Jain, 1989; Baxter & Jain, 1991).

Assuming targeted nanocarriers successfully overcome these drawbacks, the system has often to be taken up by targeted cancer cells to be effective. Several studies have shown that the cellular uptake of NPs can depend on many factors, including biological features. This is the case of the proven role of cell cycling not only on uptake rate but also on the amount of nanocarriers internalized by cells (Kim *et al.,* 2012). In fact, internalized nanocarriers are not exported by cell but are split between daughter cells when the parent cell divides. Thus, in a cell population, the dose of internalized nanocarriers in each cell significantly varies as the cell advances throughout the cell cycle. In a critical perspective, more focused and dedicated approach to the understanding of the in situ (*in-vivo*) interface between engineered nanomedicines and their targets is thereby needed to transfer the remarkable possibilities of nanoscale interactions in biology into therapeutics (Mahon *et al.,* 2012). Nevertheless, some targeted nanoparticulate products, such as CALAA-01 and BIND-014, have recently entered in clinical trials.

2.8 Oral delivery of nanoparticulate system

In the past decades, the oral administration of anticancer drugs is raising great interest in the scientific community, a suggested by the growing number of drugs commercially available and by the orally formulated agents in development. In fact, oral cancer therapy provides many attractive benefits as compared to parenteral routes, such as the low cost and the ease of administration, associated to great convenience and life quality of the patients (Malingre *et al.,* 2001; Bebaw & Sze, 2008). Nevertheless, the systemic efficacy of orally administered anticancer drugs is seriously compromised by their poor oral bioavailability.

Before the drug molecule reaches its final destination, it must go through the stomach, the lumen of the intestine, the mucus layer coating the intestinal epithelium and, finally, the epithelium itself. Both the highly acidic condition in the stomach as well as the digestive enzymes that are secreted along the entire gastrointestinal (GI) tract can potentially degrade the drug before it moves

across the epithelium. Furthermore, numerous chemotherapeutics show low permeability across GI mucosa, due to not only the limited solubility and structural instability in GI fluids, but also the affinity for intestinal and liver cytochrome P450 metabolic enzymes (first-pass extraction mechanism) and to the P-glycoprotein (P-gp) involved in MDR (Malingre *et al.,* 2001; Bebaw & Sze, 2008). Adhesion and diffusion of the drug in the mucosal microenvironment of the GI tract represent another important challenge in oral chemotherapy. In fact, GI tract is covered by a mucus layer, which is a very complex protection systems from the pathogens and foreign agents and has been highlighted as a significant barrier for drug penetration (Atuma *et al.,* 2001). Finally, the drug transport across GI epithelium can occur through: i) the paracellular transport, which depends from the opening of tight junctions, ii) the transcellular transport by active endocytic mechanism, such as pinocytosis and clathrin-mediated endocytosis and iii) the lymphatic mediated transport, which is achieved preferentially after absorption by M cells, relatively less protected by mucus and characterized by a high transcytotic activity (Cai *et al.,* 2010).

Nanotechnology engineering of chemotherapeutics represents an interesting approach in order to overpass the limits related to systemic oral administration of anticancer drugs. In particular, nanocarriers provide the adequate size and possibly the appropriate surface modification to improve drug permeation across GI mucosa and absorption by the intestinal cells as well as to reduce the P-gp efflux and the cytochrome P450-mediated inactivation (Mei *et al.,* 2013; Feng, 2004).

2.8.1 Improving drug permeation across GI mucosa

Particle size and size distribution are considered crucia parameters to optimize drug absorption and distributions, as well as to minimize the toxicity, of the encapsulated drug (Cai *et al.,* 2010; Mei *et al.,* 2013). Particles smaller than 100 nm may allow significant drug penetration across the intestinal mucosa, whilst the oral administration of particles with a diameter of 500 nm may lead to the permeation of a percentage of the administrated dose as low as 10%.

Furthermore, if 1 μm particles can be especially accumulated in the Peyer's patches, no permeation at the lymphoid tissues was observed with particles of higher size (Cai *et al.,* 2010). On the other hand, it has been reported that 100 nm particles may diffuse also through the submucosal layer, allowing a systemic distribution, while larger nanocarriers predominantly localize in the epithelial lining of the tissue (Desai *et al.,* 1997).

Although the correlation between particle size and GI mucosa barrier permeation is often unclear and involves unknown mechanisms, the basic criteria that particle size <500 nm are preferred in order to optimize cell uptake and to enhance drug bioavailability after oral administration can be accepted (Cai *et al.,* 2010; Mei *et al.,* 2013). Nevertheless, if this cut-off diameter may be useful to optimize in-vitro uptake by GI epithelial cells, it can be sometimes detrimental for in-vivo penetration of the GI mucus layer, which represents a barrier for nanocarriers permeation (Ensign *et al.,* 2012).

To increase the persistence of a nanocarrier at GI mucosa, surface engineering is required so as to cross the loosely adherent mucus layer, which is continuously removed by peristalsis and replaced, and to reach the firmly adherent layer, which is deposed on GI epithelium (Ensign *et al.,* 2012). As described in the case of lung delivery, nanocarrier surface can be modified to enhance or reduce adhesion to mucus layer. The use of mucoadhesive polysaccharides, such as chitosan or alginate, has been widely employed to effectively engineer nanocarriers for drug delivery to GI mucosal tissues (Ensign *et al.,* 2012). In particular, through electrostatic interactions with mucus components, mucoadhesive nanocarriers can penetrate across the mucus layer and increase the contact between encapsulated drug and the surface of absorptive cells, enhancing drug permeation (Chakravarthi & Robinson, 2011). In some cases, such as for chitosan based nanoparticles, improved drug permeation across GI barrier was related not only to the mucoadhesive properties but also to an opening effect on the tight junction (Saremi *et al.,* 2011).

2.8.2 Increasing drug resistance toward GI harsh environment and MDR effect

Taking into account the variety of conditions expressed in the GI tract, especially the variable pH value, strategies based on polymers enhancing the stability of the delivery system at low pHs or releasing drugs in a pH-dependent fashion are required. An interesting strategy to overcome nanocarrier degradation in stomach relies in the development of polymeric nanocarriers, in which biodegradable nanocarriers are protected by a coating based on polymers stable at low pH while dissolving at pH 5-6 of small intestine, such as alginates (Kanwar *et al.,* 2012). This strategy, developed to overcome the harsh environment of the GI tract, acquire additional importance when looking for targeted drug delivery to GI-specific areas, such as colon. In fact, nanocarriers made of widely employed biodegradable polymers, such as poly(lactic acid) (PLA), may be embedded in polysaccharide-based hydrogels, such as alginate/chitosan hydrogels, also to actively target drugs to inflamed colonic tissues (Laroui *et al.,* 2010; Laroui *et al.,* 2013).

In addition to enhancing particle stability toward acidic pH, nanocarrier engineering for oral cancer therapy should also take into account the MDR effect exerted by the P-gp, which is extensively expressed in the GI tract (Malingre *et al.,* 2001). On this matter, nanocarriers combining mucoadhesive properties and the ability to inhibit P-gp-mediated efflux mechanism can be successfully achieved by surface chemical modification with PEG (Zabaleta *et al.,* 2012). In particular, PEG is reported to exert an inhibitory effect comparable to that obtained after the administration of verapamil, a calcium blocker and well-known inhibitor of the P-gp efflux pump employed in conventional clinical therapies (Kruijtzer *et al.,* 2002). Nevertheless, PEG molecular weight may influence nanocarrier mucoadhesion properties and, consequently, their permeation through GI mucus (Zabaleta *et al.,* 2012). On the other hand, a muco inert high-density coating of low molecular weight PEG, as observed for lung delivery, may allow the achievement of MPP that readily penetrate the loosely adherent mucus layer and enter the firmly adherent one (Ensign *et al.,* 2012).

2.9 Drug specific review

2.9.1 Curcumin

Drug: Curcumin (CUR)

IUPAC Name: 1, 7-bis-(4-hydroxy-3-methoxyphenyl)-1, 6-heptadiene-3, 5-dione

Molecular formula: $C_{21}H_{20}O_6$

Molecular Weight: 368.39 g/mol

Polarity: 3.28

Melting point: 183°C

pKa: 9.9

LogP: 3.28

Origin: Curcumin is a bis-α, β-unsaturated β-diketone, extracted from the dried root of the rhizome *Curcuma longa*. The process of extraction requires the raw material to be ground into powder, and washed with a suitable solvent that selectively extracts CUR.

Chemical structure:

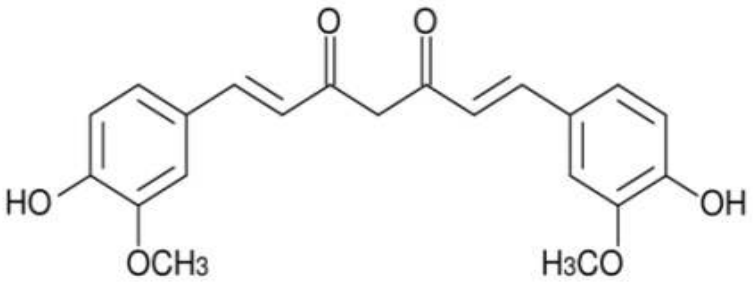

Figure 2.4 Chemical structure of curcumin

Physical properties: CUR is an orange-yellow crystalline powder.

Solubility: Practically insoluble in water. Soluble in acetonitrile, dichloromethane, DMSO, ethyl acetate, ethanol and acetone etc. The solubility of CUR in there solvents is approx. 1mg/ml and is at least 20 mg/ml in acetone. The bis-keto form predominates in acidic and neutral aqueous solutions and in the cell membrane.

Storage conditions: Stable for ≥2 years in dry solid state at room temperature.

Stability: CUR is unstable at basic pH, and degrades within 30 min to Trans-6-(4'-hydroxy-3'-methoxyphenyl)-2,4-dioxo-5-hexanal,ferulicacid,feruloylmethane and vanillin (Lin *et al.,* 2000). The presence of foetal calf serum or human blood, or addition of antioxidants such as ascorbic acid, N-acetylcysteine or glutathione, completely blocks this degradation in culture media or phosphate buffer above pH 7 (Wang *et al.,* 1997). Under acidic conditions, the degradation of CUR is much slower, with less than 20% of total CUR decomposed at 1 hr (Wang *et al.,* 1997). Other investigators have also found that CUR is more stable in cell culture medium containing 10% foetal calf serum or in human blood, with less that 20% decomposition within 1 hr compared to 90% within 30 min in serum-free medium (Wang *et al.,* 1997).

Mechanism of Action:

- ✓ Increases Nrf2 protein and modulates phase II enzyme expression in B(a)P-treated mice
- ✓ Decreases TPA-induced protein kinase C translocation and effects TPA-induced molecular alterations in mouse skin
- ✓ Inhibits NF-kB and STAT3 signaling and induces apoptosis

Therapeutic indications: CUR is reported of having antioxidant, anti-inflammatory, fungicidal, antimicrobial, anti-cancer activities, hepato and nephro-protective, thrombosis suppressing, myocardial infarction protective, hypoglycemic and antirheumatic activities (Wang *et al.,* 1997).

Pharmacokinetics:

Absorption

One of the major observations related to CUR studies involves the observation of extremely low serum levels. The first reported study to examine the uptake, distribution, and excretion of CUR was by Wahlstrom and Blennow in 1978 using Sprague–Dawley rats. Negligible amounts of CUR in blood plasma of rats after oral administration of 1 g/kg of CUR showed that CUR was poorly absorbed from the gut (Wahlstrom & Blennow, 1978). In 1980, Ravindranath *et al.* showed that after oral administration of 400 mg of CUR to rats, no CUR was found in heart blood, whereas a trace amount (<5 μg/ml) was found in the portal blood from 15 min to 24 hr after administration of CUR (Ravindranath & Chandrasekhara, 1980). In another study using tritium-labeled CUR, the same group showed detectable amounts of CUR in blood with doses ranging from 10-400 mg of CUR per animal (Ravindranath & Chandrasekhara, 1981). When CUR was given orally at a dose of 2 g/kg to rats, a maximum serum concentration of 1.35±0.23 μg/ml was observed at time 0.83 hr, whereas in humans the same dose of CUR resulted in either undetectable or extremely low (0.006±0.005 μg/ml at 1 hr) serum levels (Shoba *et al.,* 1998). A very recent study by Yang *et al.* showed that 10 mg/kg of CUR given i.v. in rats gave a maximum serum CUR level of 0.36±0.05μg/ml, whereas a 50-fold higher CUR dose administered orally gave only 0.06±0.01μg/ml maximum serum level in rat (Yang *et al.,* 2007).

Distribution

Ravindranath *et al.* showed that after oral administration of 400 mg of CUR to rats only traces of unchanged drug were found in the liver and kidney. At 30 min, 90% of CUR was found in the stomach and small intestine, but only 1% was present at 24 hr (Ravindranath & Chandrasekhara, 1980). In an *in-vitro* study, when everted sacs of rat intestine were incubated with 50-750 μg of CUR in 10 ml of incubation medium 30-80% of the CUR disappeared from the mucosal side and no CUR was found in the serosal fluid. Less than 3% of the CUR was found in the tissues at the highest CUR concentration.

Biological half-life

The absorption and elimination half-lives of orally administered CUR (2 g/kg) in rats were reported to be 0.31±0.07 and 1.7±0.5 hr, respectively. But in humans, the same dose of CUR did not allow the calculation of these half-life values because the serum CUR levels were below the detection limit at most of the time points in most of the experimental subjects (Shoba *et al.,* 1998).

A lower CUR dose of 1 g/kg administered orally in rats was found to have an elimination half-life value of 1.45 hr, (Maiti *et al.,* 2007) which is not significantly different from the half-life reported for a higher CUR dose and may be indicative of dose independency of CUR elimination half-life in rats. The elimination half-life values for i.v. (10 mg/kg) and oral (500 mg/kg) CUR in rats were reported to be 28.1±5.6 and 44.5±7.5 hr, respectively (Yang *et al.,* 2007). However, the existing evidence in literature is not enough to conclude about the factors controlling in vivo elimination half-life of CUR and future studies are warranted to address this issue.

Metabolism

Liver was indicated as the major organ responsible for metabolism of CUR (Garcea *et al.,* 2004; Hoehle *et al.,* 2006; Wahlstrom & Blennow, 1978). Holder *et al*. reported that the major billiary metabolites of CUR are glucuronides of tetrahydrocurcumin (THC) and hexahydrocurcumin (HHC) in rats. A minor biliary metabolite was dihydroferulic acid together with traces of ferulic acid (Holder *et al.,* 1978). In addition to glucuronides, sulfate conjugates were found in the urine of CUR treated rats (Ravindranath & Chandrasekhara, 1980). Hydrolysis of plasma samples with glucuronidase by Pan *et al.* showed that 99% of CUR in plasma was present as glucuronide conjugates. This study also revealed curcumin-glucuronoside, dihydrocurcumin-glucuronoside, tetrahydrocurcumin (THC)-glucuronoside, and THC are major metabolites of CUR *in vivo* (Pan *et al.,* 1999). These results are in agreement with Ireson *et al.* who examined CUR metabolites in rat and human (Ireson *et al.,* 2001). Asai *et al.* evaluated the absorption and metabolism of orally administered CUR in rats. The

enzymatic hydrolysis of plasma samples showed that the predominant metabolites in plasma following oral administration were glucuronides/sulfates of CUR.

Elimination

Systemic elimination or clearance of CUR from the body is also an important factor, which determines its relative biological activity. An early study by Wahlstrom and Blennow reported that when 1 g/kg CUR was given orally to rats, 75% of it was excreted in the feces and negligible amounts were found in the urine. Intravenous and i.p. administration of CUR resulted in biliary excretion of drug from cannulated rats (Holder *et al.,* 1978). Another study using radiolabeled CUR showed that when drug was administered orally to rats at a dose of 400 mg/rat, nearly 40% of CUR in unchanged form was found in the feces. Though no detectable amount of CUR was found in urine, some of the derivatives like CUR glucuronide and sulfates were observed. The major route of elimination of the radio labeled products was through feces; urinary excretion of the label was very low regardless of the dose

Toxicological profile of CUR

Studies of CUR in animals have confirmed a lack of significant toxicity since an early report in which doses up to 5 g/kg were administered orally to Sprague-Dawley rats (Wahlstrom & Blennow, 1978). Systematic preclinical studies funded by the Prevention Division of the US National Cancer Institute did not discover adverse effects in rats, dogs or monkeys of doses up to 3.5 g/kg body weight (BW) administered for up to 3 months (NCI, 1996). One report of dietary CUR suggested ulcerogenic activity in the stomach of the albino rat (Gupta *et al.,* 1980), but this finding has not been confirmed in subsequent studies. In more recent preclinical studies of CUR, no toxicity has been observed from 2% dietary CUR (approximately 1.2 g/kg BW) administered to rats for 14 days (Sharma *et al.,* 2001) or from 0.2% dietary CUR (approximately 300 mg/kg BW) administered to mice for 14 weeks (Perkins *et al.,* 2002).

2.9.2 Naringenin

Drug: Naringenin (NAR)

IUPAC Name: 2,3-dihydro-5,7-dihydroxy-2-(4-hydroxyphenyl)-4H-benzopyran 4-one

Molecular formula: $C_{15}H_{12}O_5$

Molecular Weight: 272.26 g/mol

Melting point: 254°C

pKa: 7.91

LogP: 2.52

Origin: Naringenin (4′,5,7-trihydroxyflavanone), a natural flavonoid aglycone of naringin, is widely distributed in citrus fruits, tomatoes, cherries, grapefruit and cocoa.

Chemical structure:

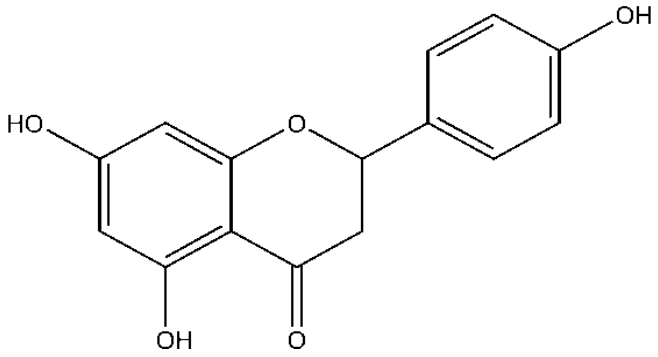

Figure 2.5 Chemical structure of naringenin

Physical properties: NAR is a white-crystalline powder.

Solubility: Naringenin is almost insoluble in water and is soluble in organic solvents such as alcohol, ethyl acetate, acetonitrile, methanol and DMSO, etc.

Storage conditions: Stable for ≥2 years in dry solid state at room temperature.

Mechanism of Action

- ✓ Activation of phase II detoxifying enzymes 53
- ✓ Against UVB-induced apoptosis and enhances the removal of cyclobutane pyrimidine dimers in keratinocytes

Therapeutic indications

As a well-known antioxidant compound, the bioactivity of NAR has been attributed to its structure-activity relationship. The number of hydroxyl substitutions of NAR can donate hydrogen to ROS, allowing acquisition of stable structure, thus enabling scavenging of these free radicals (Shen *et al.,* 2004 & Heo *et al.,* 2004). In addition, NAR has also been extensively investigated for its pharmacological activities, including antitumor (Kanno *et al.,* 2005), anti-inflammatory (Hirai *et al.,* 2007), and hepatoprotective (Lee *et al.,* 2004) effects. Although NAR possesses excellent free radical scavenging ability.

Pharmacokinetics

As NAR is generally present in foods bound to sugars as β-glycosides (i.e., naringin), it was originally thought that absorption from the diet would be negligible. However, a number a studies have detected NAR in human urine (Ameer *et al.,* 1996; Fuhr & Kummert, 1995; Ishii *et al.,* 1997, Lee & Reidenberg, 1998; Weintraub *et al.,* 1995) and plasma (Ameer *et al.,* 1996; Fuhr & Kummert, 1995) following oral doses of pure naringin (Ameer *et al.,* 1996; Ishii *et al.,* 1997) or grapefruit juice (Ameer *et al.,* 1996; Fuhr & Kummert, 1995; Lee & Reidenberg, 1998; Weintraub *et al.,* 1995). Hesperetin has been detected also in human urine (Ameer *et al.,* 1996; Weintraub *et al.,* 1995) and plasma (Ameer *et al.,* 1996) following doses of pure compound or orange juice. These results showed that NAR and hesperetin can be absorbed from the diet. In fact, studies using 3-[^{14}C]-hesperetin in rats indicate that intestinal absorption of aglycone flavanones may be greater than 90% (Honohan *et al.,* 1976).

The glycoside form of NAR and naringin, is not detected in either human or animal urine suggesting that naringin is deglycosylated prior to intestinal absorption. It has been shown that the intestinal microflora of rats (Booth *et al.,* 1958; Griffiths *et al.,* 1972) and humans (Fuhr & Kummert, 1995; Hodgson *et al.,* 1998) can cleave the glycosidic bonds of naringin, liberating the aglycone form NAR. Studies by Furh *et al.* (Fuhr & Kummert, 1995) have shown large inter individual differences in the ability of humans to convert naringin to NAR as evident in feces, suggesting that the presence or absence of certain bacterial strains in the gut may explain the inter individual variability observed in studies examining grapefruit-juice-drug interactions (Bailey *et al.,* 1991). In a recent study, Kim et al. (Hodgson *et al.,* 1998) identified a number of bacteria in the human intestine that are capable of transforming naringin to NAR and hesperidin to hesperetin, including Fusobacterium K-60, Eubacterium YK-4, and Bacteroides JY-6.

Intestinal microflora have been shown to further metabolize NAR. Booth et al. (Booth *et al.,* 1958) originally showed that oral doses of naringin administered to rats yielded 4 hydroxyphenyl propionic acid, 4-hydroxycinnamic acid, and 4-hydroxybenzoic acid sulfate in the urine. Griffiths and Smith (Griffiths *et al.,* 1972) showed that rat intestinal microflora resulted in the generation of 4-hydroxyphenylpropionic acid and NAR only, suggesting that 4-hydroxycinnamic acid and 4-hydroxybenzoic acid may be metabolites that are generated by hepatic enzymes. Honohan *et al.* (Honohan *et al.,* 1976) showed that the major intestinal metabolite of 3-[^{14}C] hesperetin in rats was 3-phenylpropionic acid, while hepatic enzymes mediated further breakdown to benzoic acid and CO_2. More recently, Kim *et al.* have shown that human intestinal bacteria can metabolize naringin to NAR and then to 4-hydroxybenzoic acid, phloroglucinol, 2,4,6-trihydroxybenzoic acid, and 4-hydroxyphenylacetic acid, demonstrating species differences in the intestinal metabolism of naringin and NAR.

A large percentage of NAR absorbed in humans appears in the urine as NAR glucuronides (Fuhr & Kummert, 1995; Ishii *et al.,* 1997; Lee & Reidenberg 1998), indicating that conjugation, presumably within the intestine or liver (Fuhr

& Kummert, 1995), may play a major role in the metabolism of this compound. NAR has also been reported to be a substrate for a UDP glucuronosyl transferase (Green *et al.,* 1998). Furh *et al.* (Fuhr & Kummert, 1995) showed that excretion of NAR glucuronides in humans reaches levels more than 100-fold higher than the concentration of NAR excreted in the urine. Hackett *et al.* (Hackett *et al.,* 1979) have shown that a major route for flavonoid metabolism in rats is excretion in the bile. This generally occurs following conjugation of flavonoid polar hydroxyl groups with glucuronic acid, sulfate, or glycine. NAR present in the bile may either be excreted or reabsorbed, therefore raising the possibility of enterohepatic recycling of NAR. In addition to conjugation, NAR may be further metabolized by hepatic enzymes. Nielsen *et al.* (Nielsen *et al.,* 1998) have recently examined the metabolism of NAR and hesperetin in rat liver microsomes. The major metabolite observed for both NAR and hesperetin was the flavonoid eriodictyol. Eriodictyol was generated by the addition of a hydroxyl group to the R_6 position of NAR and the demethylation of the R_6 methoxy of hesperetin. The hydroxylation of NAR was shown to be mediated by hepatic cytochrome P450 1A (CYP1A) (Nielsen *et al.,* 1998).

NAR has been detected in the plasma following oral administration of naringin or grapefruit juice but is generally reported to be below accurate detection limits (Ameer *et al.,* 1996; Fuhr & Kummert, 1995) and has not been reported to exceed 4 mM (Fuhr & Kummert, 1995). However, due to the lipophilic nature of NAR, it is possible that it accumulates within tissues, particularly membranes, and eventually reaches greater concentrations than those observed in the plasma. This accumulation would most likely occur in tissues such as the liver and intestine. In support of this, it has been demonstrated that approximately 40% of a dose of hesperetin,-3-[14C] given either orally or intraperitoneally to rats, was recovered as $^{14}CO_2$, a by-product of hepatic metabolism (Honohan *et al.,* 1976). This suggests that at least 40% of the hesperetin dose reached the liver.

Toxicological profile of NAR

Toxicity studies of NAR are scarce; however, flavonoids are generally considered to have low toxicity. In one study (Booth *et al.,* 1958), a single 2 g oral dose of NAR was administered to a human volunteer with no deleterious effects. NAR has also been administered to humans at oral doses of 500 mg with no adverse responses (Ameer *et al.,* 1996; Ishii *et al.,* 1997). Kim *et al.* have reported on the *in-vitro* cytotoxicity for various flavonoids in a number of cells lines. The IC_{50} (50% inhibition concentration) for cell growth was >1 mM for both NAR and hesperetin in the human hepatoma cell line $HepG_2$, the Macacus' rhesus monkey kidney cell line MA-104, and the human lung cancer cell line A549. The results of these studies indicate that these flavonoids have relatively low toxicity in cell culture.

2.10 Polymer specific review

2.10.1 Soluthin MD®

The Soluthin MD® (SMD) is an approved new class of lipopolysaccharide based hydrophilic compound, composed of major carbohydrate component, 80% maltodextrin and minor lipid component 20% phosphatidylcholine as shown in Figure 2.4. SMD act as solubilizer, bioavailability enhancer, biodegradable and biocompatible carrier (Chen & Chen, 2012). Maltodextrin of SMD are complex mixtures of glucose, disaccharides and polysaccharides obtained by the partial hydrolysis of starch, that have the ability to form amorphous glassy matrices during the encapsulation process via a phenomenon "host-guest" (Kilburn *et al.,* 2005). The conformational change from a flexible coil to a helix form in the presence of a guest, which depends on the size of the encapsulating molecules, is believed to be essential for interactions to occur (Soini *et al.,* 1994). These properties can be utilized for loading and encapsulation of variety of poorly water soluble drugs in the form of nanocarriers for enhancing oral bioavailability as well as anticancer efficacy.

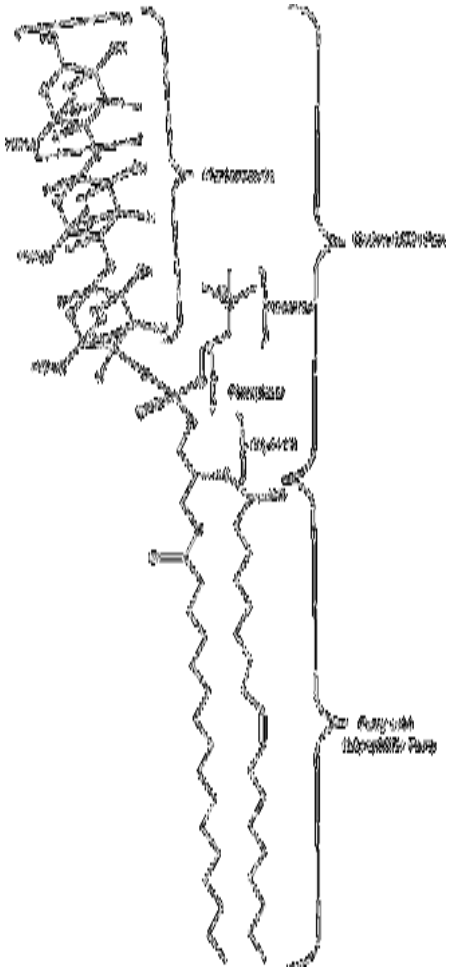

Figure 2.6 Structure of lipopolysaccharide (Soluthin MD®); SMD consists of following regions: from the bottom, lipophillic part, hydrophilic part (glycerol, phosphate, choline) including maltodextrin, which consists of repeating units (denoted in brackets, with an "n") of polysaccharides.

Appearance

Aggregation state: Powder (flowable)

Colour: Beige

Odour: Odourless

Storage: Store in cool place at not more than 8°C.

Solubility: Soluble in water, ethanol (95%), other organic solvents, and neutral to alkaline solutions at pH>6.5.

Safety: Nontoxic and non irritant material, biocompatible with healthy and infected skin, biodegradable.

2.10.2 Eudragit® E 100

The Eudragit® E100 (EE100) cationic copolymer consisting of 1:2:1 ratio of methyl methacrylate, N,N-dimethylaminoethyl methacrylate and butyl methacrylate monomers, has been widely employed to improve solubility of poorly water-soluble drugs (Jung *et al.,* 1999). As it possesses basic sites of dimethylamino groups which ionize in the gastric fluid and makes it easy to dissolve in the gastric environment (Wang *et al.,* 2004).

Chemical structure:

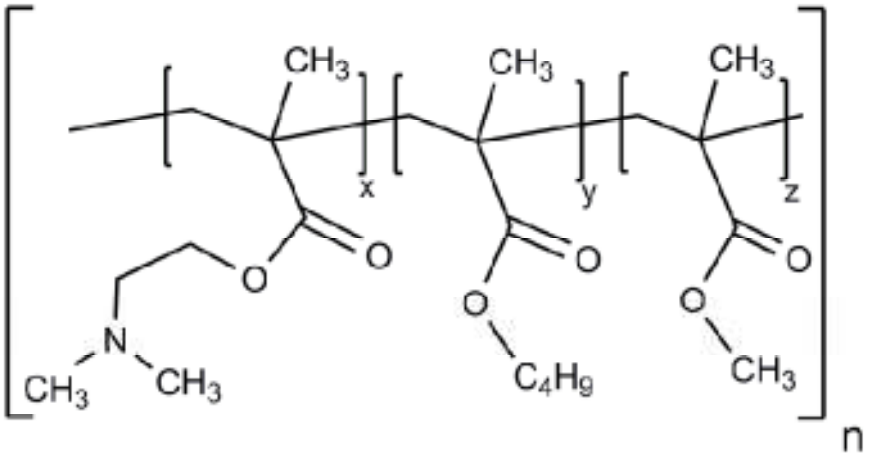

Figure 2.7 Chemical structure of Eudragit® E 100

Molecular weight: Based on SEC method the weight average molar mass (Mw) of Eudragit® E 100 is approximately 47,000 g/mol.

Characters

Description: Eudragit® E 100 is colourless to yellow tinged granules with a characteristic amine-like odour.

Solubility: 1 g of Eudragit® E 100 dissolves in 7 g methanol, ethanol, isopropyl alcohol, acetone, ethyl acetate, methylene chloride or 1 N hydrochloric acid to give clear to slightly cloudy solutions. The solid substance is practically insoluble in petroleum ether and water.

Viscosity/Apparent viscosity: 3 - 6 mPa . s

Viscosity/Kinematic viscosity: 2.5 - 5.5 mm^2/s

Refractive index: 1.380 - 1.385

Relative density: 0.811 - 0.821

Storage: Protect from warm temperatures (USP, General Notices). Protect from moisture. Any storage between 8°C and 25°C fulfils this requirement. Eudragit® E 100 tends to form lumps at warm temperatures (≥30°C). This has no influence on the quality. The lumps are easily broken up again.

Stability: Minimum stability dates are given on the product labels and batch-related Certificates of Analysis. Storage Stability data are available upon request.